

# Angiogenic Oligosaccharides of Hyaluronan Induce Multiple Signaling Pathways Affecting Vascular Endothelial Cell Mitogenic and Wound Healing Responses\*

Received for publication, October 1, 2001, and in revised form, August 22, 2002  
Published, JBC Papers in Press, August 22, 2002, DOI 10.1074/jbc.M109443200

Mark Slevin<sup>‡§</sup>, Shant Kumar<sup>¶</sup>, and John Gaffney<sup>‡</sup>

From the <sup>‡</sup>Department of Biological Sciences, Manchester Metropolitan University, Manchester M1 5GD, United Kingdom and the <sup>¶</sup>Department of Pathological Sciences, Stopford Building, Manchester Victoria University, Manchester M1 5GD, United Kingdom

Hyaluronan (HA) is a large nonsulfated glycosaminoglycan and an important regulator of angiogenesis, in particular, the growth and migration of vascular endothelial cells. We have identified some of the key intermediates responsible for induction of mitogenesis and wound recovery. Treatment of bovine aortic endothelial cells with oligosaccharides of hyaluronan (o-HA) resulted in rapid tyrosine phosphorylation and plasma membrane translocation of phospholipase C $\gamma$ 1 (PLC $\gamma$ 1). Cytoplasmic loading with inhibitory antibodies to PLC $\gamma$ 1, G $\beta$ , and G $\alpha_{i/o/t/z}$  inhibited activation of extracellular-regulated kinase 1/2 (ERK1/2). Treatment with the G $\alpha_{i/o}$  inhibitor, pertussis toxin, reduced o-HA-induced PLC $\gamma$ 1 tyrosine phosphorylation, protein kinase C (PKC)  $\alpha$  and  $\beta$ 1/2 membrane translocation, ERK1/2 activation, mitogenesis, and wound recovery, suggesting a mechanism for o-HA-induced angiogenesis through G-proteins, PLC $\gamma$ 1, and PKC. In particular, we demonstrated a possible role for PKC $\alpha$  in mitogenesis and PKC $\beta$ 1/2 in wound recovery. Using antisense oligonucleotides and the Ras farnesylation inhibitor FTI-277, we showed that o-HA-induced bovine aortic endothelial cell proliferation, wound recovery, and ERK1/2 activation were also partially dependent on Ras activation, and that o-HA-stimulated tyrosine phosphorylation of the adapter protein Shc, as well as its association with Sos1. Binding of Src to Shc was required for its activation and for Ras-dependent activation of ERK1/2, cell proliferation, and wound recovery. Neither Src nor Ras activation was inhibited by pertussis toxin, suggesting that their activation was independent of heterotrimeric G-proteins. However, the specific Src kinase inhibitor PP2 inhibited G $\beta$  subunit co-precipitation with PLC $\gamma$ 1, suggesting a possible role for Src in activation of PLC $\gamma$ 1 and interaction between two distinct o-HA-induced signaling pathways.

Angiogenesis, the formation of new blood vessels, is essential for the growth and repair of tissues and is prevalent in a variety of pathological conditions. Excessive vascularization occurs in rheumatoid arthritis, diabetic retinopathy, psoriasis, and neoplasia (1, 2). Conversely, in myocardial infarction and cerebrovascular diseases such as stroke, there is considerable destruction of the vasculature (3). Further knowledge of the

mechanisms that regulate angiogenesis is required for the development of strategies to control it.

Hyaluronan (HA)<sup>1</sup> is a nonsulfated, linear glycosaminoglycan, consisting of repeating units of ( $\beta$ ,1–4)-D-glucuronic acid-( $\beta$ ,1–3)-N-acetyl-D-glucosamine. HA is found in its native state as a high molecular mass polymer (>10<sup>6</sup> kDa) in the extracellular matrix of almost all animal tissues and in significant quantities in the skin (dermis and epidermis), brain, and central nervous system (4). Apart from its role as an inert viscoelastic lubricant, essential for healthy joint function (5), HA has a crucial role in regulation of the angiogenic process. In particular, HA is a potent regulator of vascular endothelial cell (EC) function. Native high molecular weight HA is anti-angiogenic, inhibiting EC proliferation and migration (6–8) as well as capillary formation in a three-dimensional collagen gel model (9), whereas degradation products of specific size (3–10 disaccharide units; o-HA) stimulate EC proliferation (10–11), migration (12), sprout formation (13), and result in angiogenesis in the chick chorioallantoic membrane (14) and in myocardial infarction (15). Generation of this “angiogenic” o-HA from the naturally occurring HA polymer is mediated by the endoglycosidase hyaluronidase (16), in association with tissue damage, inflammatory disease, and in certain tumors (10, 16, 17). In addition, the degree of invasiveness and metastasis of some tumors has been specifically linked to elevated HA expression (18–20). Hyaluronidase produced by tumor cells could induce angiogenesis and be used by tumor cells as a “molecular saboteur” to depolymerize HA to facilitate invasion (21). Hyaluronan was intrinsically associated with metastasis in prostate and bladder cancer (22–24) although high levels of o-HA were shown in children with a bone-metastasizing variant of renal tumor (25).

The biological functions of HA/o-HA are thought to be initiated through cell surface receptors or HA-binding proteins, resulting in signal transduction activation and ultimately mitogenesis (26–28). Native HA binds to a 34-kDa member of the hyaladherins, and increases general protein tyrosine phosphorylation and that of PLC $\gamma$ 1 in a variety of cell lines, although the role of this protein in mediating cell behavioral effects is unknown (27). o-HA-induced Ras-dependent activation of mitogen-activated protein (MAP) kinase was shown in rat embryonic 3Y1 fibroblasts (29). In T24 bladder carcinoma cells, o-HA

\* The costs of publication of this article were defrayed in part by the payment of page charges. This article must therefore be hereby marked “advertisement” in accordance with 18 U.S.C. Section 1734 solely to indicate this fact.

§ To whom correspondence should be addressed. Fax: 0161247-6365; E-mail: m.a.slevin@mmu.ac.uk.

<sup>1</sup> The abbreviations used are: HA, hyaluronan; EC, endothelial cells, o-HA, oligosaccharides of hyaluronan; MAP, mitogen-activated protein kinase; RHAMM, receptor for hyaluronan mediated motility; ERK1/2, extracellular signal-regulated kinase; BAEC, bovine aortic endothelial cells; PLC, phospholipase C; FITC, fluorescein isothiocyanate; SPM, serum poor medium; PBS, phosphate-buffered saline; FACS, fluorescence-activated cell sorter; <sup>p</sup>ERK, phospho-ERK-1/ERK-2.

induced activation of NF- $\kappa$ B via CD44 in a pathway involving Ras, protein kinase C (PKC)  $\zeta$ , and a complex containing I $\kappa$ B kinase 1 and 2 (30). In vascular EC, both CD44 (31, 32) and RHAMM (receptor for HA mediated motility) (33) have been identified as potential targets for transduction of o-HA-induced mitogenesis. Inhibition of the CD44/o-HA interaction using anti-CD44 antibodies (J173) reduced proliferation and migration of calf pulmonary artery EC and human microvessel EC (HMEC-1) (34). In three types of primary human EC, o-HA bound to the RHAMM receptor and induced tyrosine phosphorylation of p125<sup>FAK</sup>, paxillin, and p42/44 extracellular signal-regulated kinase (ERK1/2) resulting in cell proliferation (33). We have previously demonstrated that o-HA but not native HA induced up-regulation of the immediate early response genes *c-jun*, *junB*, *Krox 20*, *Krox 24*, and *c-fos* in bovine aortic EC (BAEC) (11, 35). Similarly, o-HA induced a rapid CD44-dependent activation of multiple isoforms of PKC ( $\alpha$ ,  $\beta$ , and  $\epsilon$ ), Raf-1 kinase, MEK-1, and ERK1/2 resulting in mitogenesis in these cells (31). These limited studies have so far failed to identify all of the key intermediates involved in transduction of the o-HA-induced mitogenic and wound recovery responses in vascular EC. This information could be important in the development of novel therapeutic strategies for treatment of angiogenic diseases. In this study, an extension of our findings from previous work (31), we have examined in detail rapid up-regulation of associated signaling proteins and have characterized the pathways responsible for o-HA-induced angiogenesis.

#### EXPERIMENTAL PROCEDURES

**Materials**—Primary monoclonal antibodies to H-Ras, anti-phosphotyrosine (PY99), and phospho-ERK-1/ERK-2 (<sup>32</sup>P-ERK1/2), polyclonal antibodies, and their specific blocking peptides against  $G\alpha_{i/o/t/z}$ ,  $G\alpha_{s/o/l/f}$ ,  $G\alpha_{q/11}$ , G $\beta$ , PLC $\gamma$ 1, PLC $\gamma$ 2, PLC $\beta$ 1–3, PLC $\delta$ 1, PKC $\alpha$ , PKC $\beta$ 1–2, PKC $\epsilon$ , Sos, Shc, and  $\alpha$ -actin as well as mouse B cell lymphoma cell lysate (WEHI-231) were obtained from Autogen Bioclear (Wiltshire, United Kingdom). PKC isoform-specific inhibitors (Go 6976 and PKC $\epsilon$  translocation inhibitor peptide), H-Ras inhibitor FTI-277, G $_q$  protein inhibitor GP antagonist-2A,  $G\alpha_{i/o}$  inhibitor pertussis toxin, and PP2 Src family inhibitor were from Calbiochem. Manufacture of phosphorothioate antisense and matching sense oligonucleotides directed to bovine PKC $\alpha$  was by VHBio (Newcastle-upon-Tyne, UK). Antisense, matching scrambled, and FITC-labeled oligonucleotides directed against bovine PKC $\beta$ 1– $\beta$ 2 and H-Ras were from Biognostik (Gottingen, Germany). Ras and ERK activity assay kits, as well as the Src substrate peptide (KVEKIGEGTYGVVYK), mouse monoclonal anti-Src family tyrosine kinase, and anti-phospho-Src antibodies were all from Upstate Biotechnology (Buckingham, UK). Thermanox plastic coverslips were from Nunc (Naperville, IL), ECL and ECL plus kits were from Amersham Biosciences (Bucks, UK) and the protein detection reagent was obtained from Bio-Rad. All other materials and chemicals were from Sigma.

**Preparation of o-HA**—The method of preparation is described in full elsewhere (14). Briefly, native rooster comb HA (500 mg) was dissolved in sodium acetate buffer (50 ml, 0.1 M, pH 5.4) containing 0.15 M NaCl and treated with 20,000 units of bovine testicular hyaluronidase at 37 °C. After 2, 4, 6, 8, and 24 h, aliquots (10 ml) were treated with 1 ml of trichloroacetic acid. Mixtures were centrifuged, and supernatants were dialyzed against distilled water for 24–48 h at 4 °C in Spectra-Por tubing (Pierce-Warriner, Chester, UK) with at least 4 changes. They were then re-centrifuged and lyophilized. The powder was dissolved in 20 ml of 0.1% acetic acid and applied to a G50 Sephadex column (2.6  $\times$  180 cm). Fractions (10 ml) were collected, assayed for uronic acid, and combined to yield three pools (F1, F2, and F3). The size range of oligosaccharides in each pool was determined after incorporation of [<sup>3</sup>H]glucosamine-labeled HA, SDS-PAGE, and fluorography, as described previously (14). Successive bands differed on SDS gels by one disaccharide unit, and precise definition of the size range was determined by comparison with labeled octa-, hexa-, and tetrasaccharides of known molecular size. F1, F2, and F3 fractions consisted of disaccharide units of >16, 10–16, and 3–10, *i.e.* of approximately >7200, 4500–7200, and 1350–4500 Da, respectively. Angiogenic activity was determined by adding freeze-dried samples of each fraction onto the chorioallantoic membrane of the chick embryo. Only fraction F3 (o-HA) produced a consistent angiogenic response (14, 36) and was used in this

study. Angiogenic activity resided only in the hyaluronate fragments, because the activity of hyaluronan preparations digested with denatured hyaluronidase and a 24-h normal digest were found to lack biological activity, suggesting that there was no contamination with vascular permeability factor. Fraction F3 was further digested with *Streptomyces* hyaluronidase, and lost its biological activity, as determined by the chorioallantoic membrane of the chick embryo assay (14).

**Isolation and Routine Culture of BAECs**—BAEC were obtained and characterized as endothelial by the presence of von Willebrand factor and the uptake of Dil-labeled acetylated low density lipoprotein, as described previously (12). They were routinely cultured in Dulbecco's modified Eagle's medium containing 15% fetal calf serum, 1.5 mM glutamine, 100 IU/ml penicillin, and 50 ng/ml streptomycin (complete medium). Culture flasks were maintained at 37 °C in a humidified atmosphere of 5% CO<sub>2</sub> and 95% air.

**Cell Proliferation Studies**—BAEC were seeded at a concentration of 2  $\times$  10<sup>4</sup>/ml in 2 ml of complete medium, in triplicate 6-well plates. After attachment, medium was replaced with serum poor medium (SPM), containing 2.5% fetal calf serum in which the cells grew at a significantly reduced rate (31). In some cases, specific enzyme inhibitors, pertussis toxin (10–500 ng/ml, 6 h), Go 6976 (1–100 nM, 24 h),  $\epsilon$ -translocation inhibitor ( $\epsilon$ ti, 1–20  $\mu$ M, 24 h), FTI 277 (100 nM to 5  $\mu$ M, 24 h), GP Ant-2A (100 nM–25  $\mu$ M, 4 h), PP2 (10 nM to 10  $\mu$ M), or sense/antisense oligonucleotides directed toward PKC $\alpha/\beta$  and H-Ras (10  $\mu$ M, 72 h) were added before incubation with o-HA (1  $\mu$ g/ml) for a further 72 h. Control wells contained appropriate concentrations of the vehicle (Me<sub>2</sub>SO or ethanol). Concentration ranges and preincubation times of inhibitors were based on previously published information and our own unpublished pilot studies.<sup>2</sup> Trypan blue exclusion studies confirmed that the inhibitors were not cytotoxic to cells at the concentrations tested (data not included) and wells treated with inhibitors without o-HA were included as controls. Fresh medium and inhibitors were added every 72 h where necessary. After 72 h, cells were washed in PBS, detached in 0.05% trypsin/PBS, and counted on a Coulter counter (Coulter Electronics, Hialeah, FL) set to a threshold of 30  $\mu$ m. Statistical significance was determined by one-way analysis of variance.

**Wound Recovery Assays (Cell Migration)**—Semiconfluent cells cultured on Thermanox plastic coverslips in 24-well plates were grown to confluence in SPM (24–48 h). Medium was replaced with Dulbecco's modified Eagle's medium containing 0.1% fetal calf serum and cells were incubated for a further 48 h with or without inhibitors/antisense reagents, in triplicate, as described above. Coverslips were washed in PBS, the cellular layer wounded using a mechanical wounder (37), rinsed again in PBS to remove loose and dislodged cells, and placed into a fresh 24-well plate containing inhibitors or the appropriate vehicles. Some coverslips were immediately fixed in 100% ethanol (time zero controls). o-HA (0.5  $\mu$ g/ml) was added to some of the wells and the plate was incubated at 37 °C for 18 h. Pilot studies demonstrated that BAEC wounded under these conditions underwent negligible proliferation up to 24 h (even in the presence of o-HA), however, cell movement resulting in wound closure was almost complete in cells treated with o-HA at this concentration after 18 h (native HA had no effect, data not shown). The coverslips were rinsed ( $\times$ 3) in PBS, fixed in 100% ethanol (5 min), and allowed to air dry. The mechanical wounder produced 11 parallel lesions 400- $\mu$ m wide across the cell monolayer. Movement of cells into the denuded area was quantified using a Seescan computerized image analysis system (Manchester, UK). Each field of view covered ~2% of the total coverslip area. For each coverslip, 10 fields of view (each ~2 mm by 1.45 mm) were examined at random. The lesion area in each field of view was measured and using the data from time 0 ( $T_0$ ), the wound area was then converted to give mean % recovery from 3 identically treated coverslips (%*r*) using the equation: %*r* = [1 – (wound area at  $T_1$ /wound area at  $T_0$ )]  $\times$  100. Where  $T_1$  is the wounded area 18 h post-injury. Statistical significance was determined by one-way analysis of variance.

**Intracellular Delivery of Inhibitory Antibodies**—Semiconfluent BAEC were cultured in 6-well plates in SPM for 48 h and the medium was replaced with Ca<sup>2+</sup>- and Mg<sup>2+</sup>-free bicarbonate buffer (pH 7.3) containing glycerol (1.2 M) at 37 °C (38, 39). Cells were placed immediately on ice for 10 min and the plasma cell membrane made transiently permeable by addition of chilled L- $\alpha$ -lysophosphatidylcholine (40  $\mu$ g/ml) for a further 7 min. Pre-warmed SPM (1 ml, 37 °C), containing 5  $\mu$ g of rabbit anti-mouse control IgG, FITC-labeled IgG, or antibodies to PLC $\gamma$ 1–2, PLC $\beta$ 1–3,  $G\alpha_{i/o/t/z}$ , G $\beta$ ,  $G\alpha_{s/o/l/f}$ , or  $G\alpha_{q/11}$  was added and the cells were incubated at 37 °C for a further 1 h. Cells regained their

<sup>2</sup> M. Slevin, S. Kumar, and J. Gaffney, unpublished data.

impermeability during this phase as determined by the recovery of trypan blue exclusion (data not shown). Uptake and cytoplasmic expression of antibodies after 1 h was confirmed by fluorescent microscopy of FITC-labeled cells, using a Leitz microscope (Leica, Bensheim, Germany) and the appropriate filter, and by FACS analysis (FACScan, BD Biosciences) following washing (PBS), trypsinization, and fixation of cells in 4% formaldehyde, PBS. After a 1-h recovery, o-HA (1  $\mu\text{g}/\text{ml}$ , 5 min) was added to some of the wells that were then washed in PBS and cell lysates were collected in 0.5 ml of ice-cold radioimmunoprecipitation (RIPA) buffer containing 10 mM Tris-HCl (pH 7.5), 50 mM NaCl, 0.5% sodium deoxycholate, 0.5% (w/v) Nonidet P-40, 0.1% SDS, 1 mM  $\text{Na}_3\text{VO}_4$ , and 5  $\mu\text{g}/\text{ml}$  aprotinin (40). After sonication, lysates were centrifuged (10,000  $\times$  g, 15 min at 4  $^\circ\text{C}$ ) and the supernatants were collected and stored at  $-70^\circ\text{C}$ .

**Use of Antisense Oligonucleotides**—Phosphorothioate oligonucleotides corresponding to bovine PKC $\beta$ 1– $\beta$ 2 and H-Ras were synthesized by Biogostik (GmbH, Gottingen, Germany) using R.A.D.A.R sequence design. Sequences of antisense nucleotides for PKC $\beta$ 1– $\beta$ 2 were 5'-TCAGCTGGAATCTAAATG and matched scrambled sense/FITC-labeled nucleotides were 5'-ACTACTACAGTAGACTAC (41), whereas H-Ras antisense nucleotides were 5'-GCTTATACTCCGCATTTG and matched sense nucleotides were 5'-GTTACTGCCTCATATTCG (42). Antisense and control sense oligonucleotides directed toward bovine PKC $\alpha$  were synthesized by VHBio (Newcastle upon Tyne, UK). Antisense sequences were 5'-GTCCTCGCCGCTCCTG-3' and sense, 5'-GTCCTCGCCGCTCCTG-3' as described elsewhere (43). Semiconfluent BAEC were cultured at 37  $^\circ\text{C}$  in 24-well plates in SPM with or without oligonucleotides (10  $\mu\text{M}/72$  h) together with LipofectAMINE 2000 (Invitrogen, 10  $\mu\text{g}/\text{ml}$ ). Cell lysates were collected at 4  $^\circ\text{C}$  in RIPA buffer (300  $\mu\text{l}$ ) and processed as described previously (31). Delivery of oligonucleotides into the cell cytoplasm was monitored by addition of FITC-labeled PKC $\alpha$  oligonucleotides (10  $\mu\text{M}$ , 4–72 h) to semiconfluent BAEC cultured on glass coverslips in SPM. Pilot studies were carried out to optimize the effects of oligonucleotides, and showed a notable reduction in specific protein expression determined by Western blotting, after 72 h exposure to 10  $\mu\text{M}$  antisense oligonucleotide.

**Western Blotting**—Semiconfluent BAEC cultured in 6- or 24-well plates in SPM (48 h) were incubated with specific enzyme inhibitors or oligonucleotides before addition of o-HA (1  $\mu\text{g}/\text{ml}$ , 2–10 min) as described previously. Total cell lysates were collected in RIPA buffer and processed as described earlier, whereas plasma cell membrane and cytoplasmic fractions were separated using a digitonin-based buffer system (31). Briefly, after washing in ice-cold PBS, cells in 6-well plates were agitated at 4  $^\circ\text{C}$  for 5 min in 300  $\mu\text{l}/\text{well}$  of ice-cold buffer containing 140 mM NaCl, 25 mM KCl, 5 mM  $\text{MgCl}_2$ , 2 mM EDTA and EGTA, 10  $\mu\text{g}/\text{ml}$  leupeptin and pepstatin, 1 mM phenylmethylsulfonyl fluoride, 20 mM Tris-HCl (pH 7.5), and 0.5  $\mu\text{g}/\text{ml}$  digitonin (44). The buffer, now containing the cytoplasmic contents was removed and stored at 4  $^\circ\text{C}$ . The remaining "membrane" fraction was again rinsed in ice-cold PBS and solubilized in 300  $\mu\text{l}$  of the same buffer containing 1% (w/v) Triton X-100. Both fractions were centrifuged (10,000  $\times$  g, 15 min at 4  $^\circ\text{C}$ ) to remove insoluble debris, and stored at  $-70^\circ\text{C}$ . Complete separation of cytoplasmic and membrane fractions was demonstrated using the lactate dehydrogenase assay. Protein concentration of cell lysates was determined using a modification of the Bradford assay (Bio-Rad) and equal quantities of protein (15  $\mu\text{g}$ ) were mixed with 2 $\times$  Laemmli sample buffer, vortex mixed, and boiled in a water bath for 15 min. Samples were separated along with prestained molecular weight markers (32,000–200,000) by 12% SDS-PAGE. Proteins were electroblotted (Hofer, Bucks, UK) onto nitrocellulose filters (1 h) and the filters were blocked for 1 h at room temperature in TBS-Tween (pH 7.4) containing 5% (w/v) de-fatted milk (PKC antibodies) or containing 1% (w/v) bovine serum albumin (all other antibodies). Filters were stained with the following primary antibodies diluted in the appropriate blocking buffer, overnight at 4  $^\circ\text{C}$  on a rotating mixer: rabbit polyclonal anti-PLC $\gamma$ 1–2, PLC $\beta$ 1–3, PLC $\delta$ 1 (1:500);  $\text{G}\alpha_{\text{q}/\text{11}}$ ,  $\text{G}\beta$ ,  $\text{G}\alpha_{\text{s}/\text{12}}$ ,  $\text{G}\alpha_{\text{q}/\text{11}}$  (1:750); PKC $\alpha$ , PKC $\beta$ 1–2, PKC $\epsilon$  (1:100); H-Ras (1:400), Shc and Sos (1:1000); mouse monoclonal antibodies to pERK1/2, Src, and phospho-Src (1:1000); phosphotyrosine PY99 (1:1500), and phospho-myelin basic protein (1:1500). After washing (5 $\times$  10 min in TBS-Tween at room temperature), filters were stained with either goat anti-rabbit or rabbit anti-mouse horseradish peroxidase-conjugated secondary antibodies diluted in TBS-Tween containing 5% (w/v) de-fatted milk (1:1000, 1 h, room temperature) with continuous mixing. After a further 5 washes in TBS-Tween, proteins were visualized using ECL chemiluminescent detection.

**Antibody Specificity Studies**—Equal concentrations of protein (15  $\mu\text{g}$ ) from cell lysates were resolved in duplicate by 12% SDS-PAGE as described above. Polyclonal antibodies (1  $\mu\text{g}/\text{ml}$ ) were incubated with or

without matching blocking peptides specific for a particular epitope (Santa Cruz) (10  $\mu\text{g}/\text{ml}$ ) overnight at 4  $^\circ\text{C}$  on a rotating mixer. Antibodies were then diluted in the appropriate blocking buffer, and identical blots were stained with antibody, with or without peptide treatment using the method described previously. Specificity of Src antibodies was assessed by comparing staining in total BAEC extracts separated by Western blotting (as described above) with positive control cell lysates (WEHI-231). We have previously characterized all remaining antibodies (31).

**Immunoprecipitation Studies**—Equal concentrations of protein from total cell lysates (100  $\mu\text{g}$  in 0.5 ml of RIPA buffer) were incubated with 2  $\mu\text{g}$  of primary antibody overnight at 4  $^\circ\text{C}$  on a rotating mixer. Antibodies were then attached to protein A/G-agarose beads (20  $\mu\text{l}$ , 30 min, 4  $^\circ\text{C}$  with continuous mixing). Alternatively, cell lysates were mixed directly with antibodies already conjugated to protein-agarose beads (Shc, PLC $\gamma$ 1, 20  $\mu\text{l}$ , overnight, 4  $^\circ\text{C}$ ). The beads were pelleted by centrifugation (13,000  $\times$  g/10 min, 4  $^\circ\text{C}$ ), the supernatant was removed, and the pellet washed 3 $\times$  in ice-cold RIPA buffer (0.5 ml). Excess buffer was removed from the beads and protein-antibody complexes were solubilized in 50  $\mu\text{l}$  of 2 $\times$  Laemmli sample buffer and subjected, in duplicate, to 12% SDS-PAGE followed by blotting as described previously. One of the blots was stained with the original immunoprecipitating primary antibody to confirm equality of protein loading.

**Determination of ERK1/2 Activity**—The assay kit was supplied by Upstate Biotechnology, and the protocol was as per the manufacturers instructions. Briefly, semiconfluent BAEC, cultured in 6-well plates in SPM (48 h), were treated with the appropriate enzyme inhibitors or neutralizing antibodies as described earlier, prior to addition of o-HA (1  $\mu\text{g}/\text{ml}$ , 5 min). ERK1/2 was immunoprecipitated from the cell lysates, attached to an agarose complex, and then incubated with a substrate mixture containing myelin basic protein. After SDS-PAGE, blots were stained with anti-myelin basic protein antibody and developed using ECL plus.

**Determination of Ras Activity**—Based on the method described previously (30), semiconfluent BAEC cultured in 6-well plates in SPM (48 h) were incubated with the appropriate enzyme inhibitors/oligonucleotides described earlier, prior to addition of o-HA (1  $\mu\text{g}/\text{ml}$ , 2–10 min). Cells were lysed in 500  $\mu\text{l}$  of a  $\text{Mg}^{2+}$  buffer (pH 7.5) containing 25 mM HEPES, 150 mM NaCl, 1% Igepal Ca-630, 10 mM  $\text{MgCl}_2$ , 1 mM EDTA, 2% glycerol, 10  $\mu\text{g}$  of leupeptin and aprotinin, and 1 mM sodium orthovanadate on ice. After centrifugation (10,000  $\times$  g/20 min, 4  $^\circ\text{C}$ ) to remove insoluble material, 500  $\mu\text{g}$  of each sample was incubated with 10  $\mu\text{l}$  of Raf-1 RBD-agarose conjugate overnight at 4  $^\circ\text{C}$  on a rotating mixer. Beads containing activated Ras were centrifuged (13,000  $\times$  g/10 min at 4  $^\circ\text{C}$ ), the supernatant was removed, and the beads were washed 3 $\times$  in 0.5 ml of the same buffer. Protein complexes were solubilized by boiling (5 min) in 50  $\mu\text{l}$  of 2 $\times$  Laemmli sample buffer and separated by 12% SDS-PAGE. Resulting blots were blocked for 1.5 h in TBS-Tween containing 5% defatted milk and stained overnight with monoclonal anti-H-Ras antibody (RAS10, 1:1000) diluted in the same buffer (4  $^\circ\text{C}$  with constant mixing). Washing, secondary horseradish peroxidase antibody staining, and protein visualization were carried out as described for the Western blots above. 10  $\mu\text{g}$  of the original cell lysate was stained with anti-H-Ras monoclonal antibody and served as a control to show total Ras content of each sample.

**Determination of Src Activity**—Semiconfluent BAEC cultured in SPM for 48 h in 6-well plates were treated with o-HA (1  $\mu\text{g}/\text{ml}$ ) for 2, 5, and 10 min or for 8 min, after preincubation for 24 h with PP2 (100 nM) or pertussis toxin (100 ng/ml). Src was immunoprecipitated in RIPA lysates under nondenaturing conditions with anti-Src monoclonal antibody (2  $\mu\text{g}/\text{sample}$ , overnight at 4  $^\circ\text{C}$ ). Bound Src was attached to protein A/G-agarose beads (20  $\mu\text{l}/\text{sample}$ , 30 min, 4  $^\circ\text{C}$ ) and the beads subsequently washed (1 $\times$ ) with RIPA buffer and then (3 $\times$ ) with Src kinase reaction buffer containing 100 mM Tris-HCl (pH 7.2), 125 mM  $\text{MgCl}_2$ , 25 mM  $\text{MnCl}_2$ , 2 mM EGTA, 0.25 mM sodium orthovanadate, and 2 mM dithiothreitol. Samples were incubated at 30  $^\circ\text{C}$  in 15  $\mu\text{l}$  of kinase buffer containing 25  $\mu\text{M}$  ATP, 1  $\mu\text{g}/\text{sample}$  of Src substrate peptide, and 10  $\mu\text{Ci}$  of [ $\gamma$ - $^{32}\text{P}$ ]ATP as described previously (45). The reaction was terminated by addition of 20  $\mu\text{l}$  of 2 $\times$  Laemmli sample buffer, the samples were boiled for 5 min, and proteins were separated by SDS-PAGE. Incorporated radioactivity was visualized by autoradiography of the dried gel. Active Src kinase enzyme (Upstate Biotech) was used as a positive control in pilot experiments used to optimize the protocol.

**Analysis of Relative Protein Concentrations**—Semiquantitative analysis of protein concentration from Western blots was carried out using a scanning densitometer (Amersham Biosciences). Results accompanying the figures are given as numerical increase or decrease compared with the control untreated cells, which were assigned an

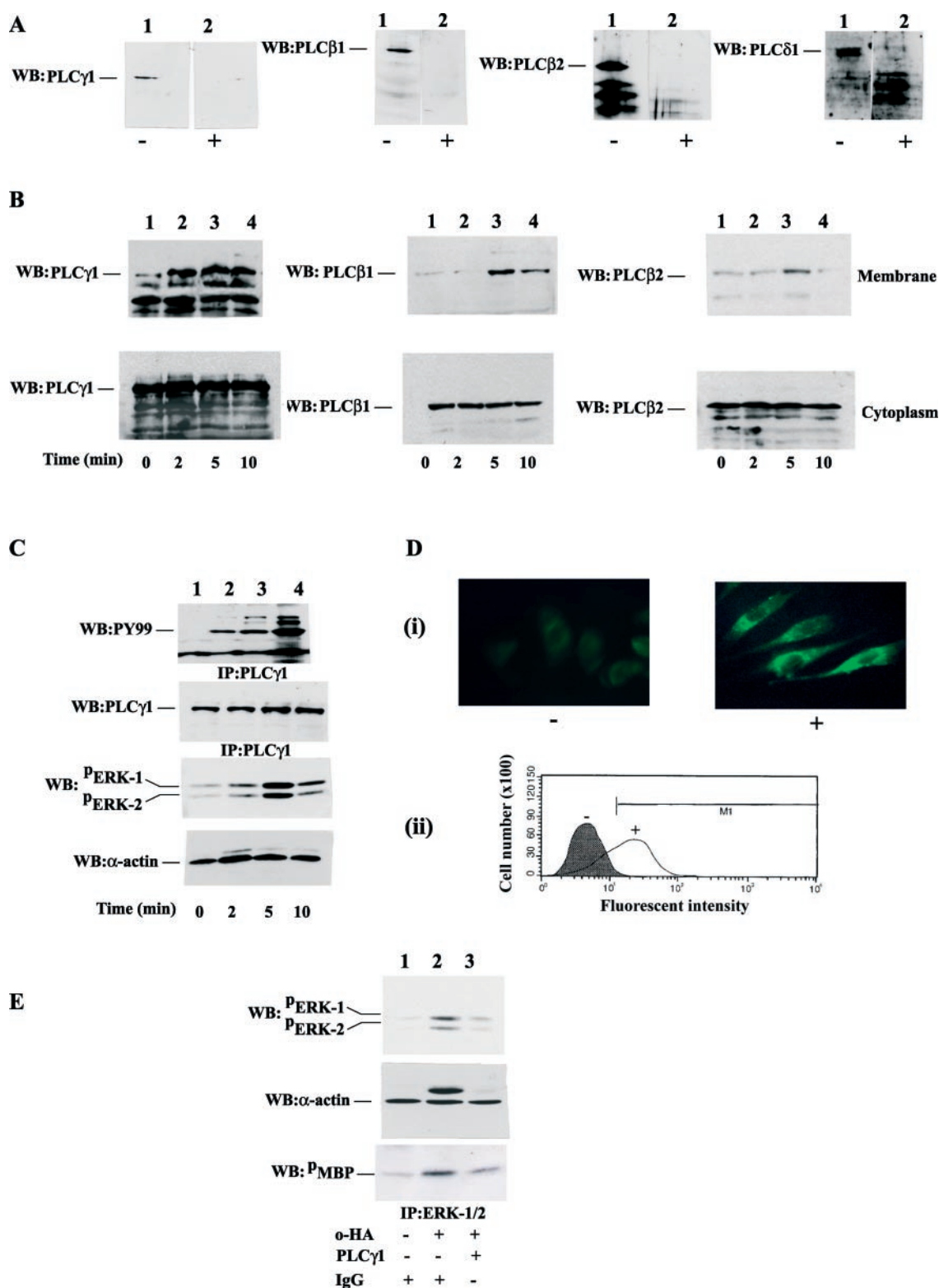


**FIG. 1. Involvement of PLC in o-HA-induced signaling.** *A*, Western blot detected expression of the  $\gamma$ 1,  $\beta$ 1,  $\beta$ 2, and  $\delta$ 1 isoforms of PLC in BAEC with (+, lane 2) and without (–, lane 1) neutralizing peptide treatment. *B*, membrane translocation of PLC $\gamma$ 1 was observed in Western blots within 2 min (lanes 2–4, left panel). Translocation of  $\beta$ 1 and  $\beta$ 2 isoforms was more transient, reaching a maximum after 5 min (lane 3, middle and right panels). *C*, Western blots showed an increase in antiphosphotyrosine staining of PLC $\gamma$ 1 (in PLC $\gamma$ 1 immunoprecipitates) increasing after 2, 5, and 10 min treatment with o-HA (1  $\mu$ g/ml) (lanes 2–4). Total PLC $\gamma$ 1 expression demonstrates equality of loading and a comparison with P-ERK1/2 expression together with  $\alpha$ -actin loading control is shown in the same samples. *D*, BAEC were made transiently permeable with *L*- $\alpha$ -lysophosphatidylcholine and loaded with FITC-labeled IgG antibodies. Delivery was monitored by (i) fluorescent microscopy where + represents permeabilized cells, and (ii) FACS analysis where M1 represents the fluorescent intensity beyond which 95% of the control cells were negative. *E*, BAEC, preloaded with anti-PLC $\gamma$ 1, antibodies (5  $\mu$ g/ml) reduced o-HA (1  $\mu$ g/ml, 5 min), and induced P-ERK1/2 expression and activity (lane 3). All experiments were carried out at least three times and a representative example is shown. WB, Western blot. MBP, myosin basic protein.

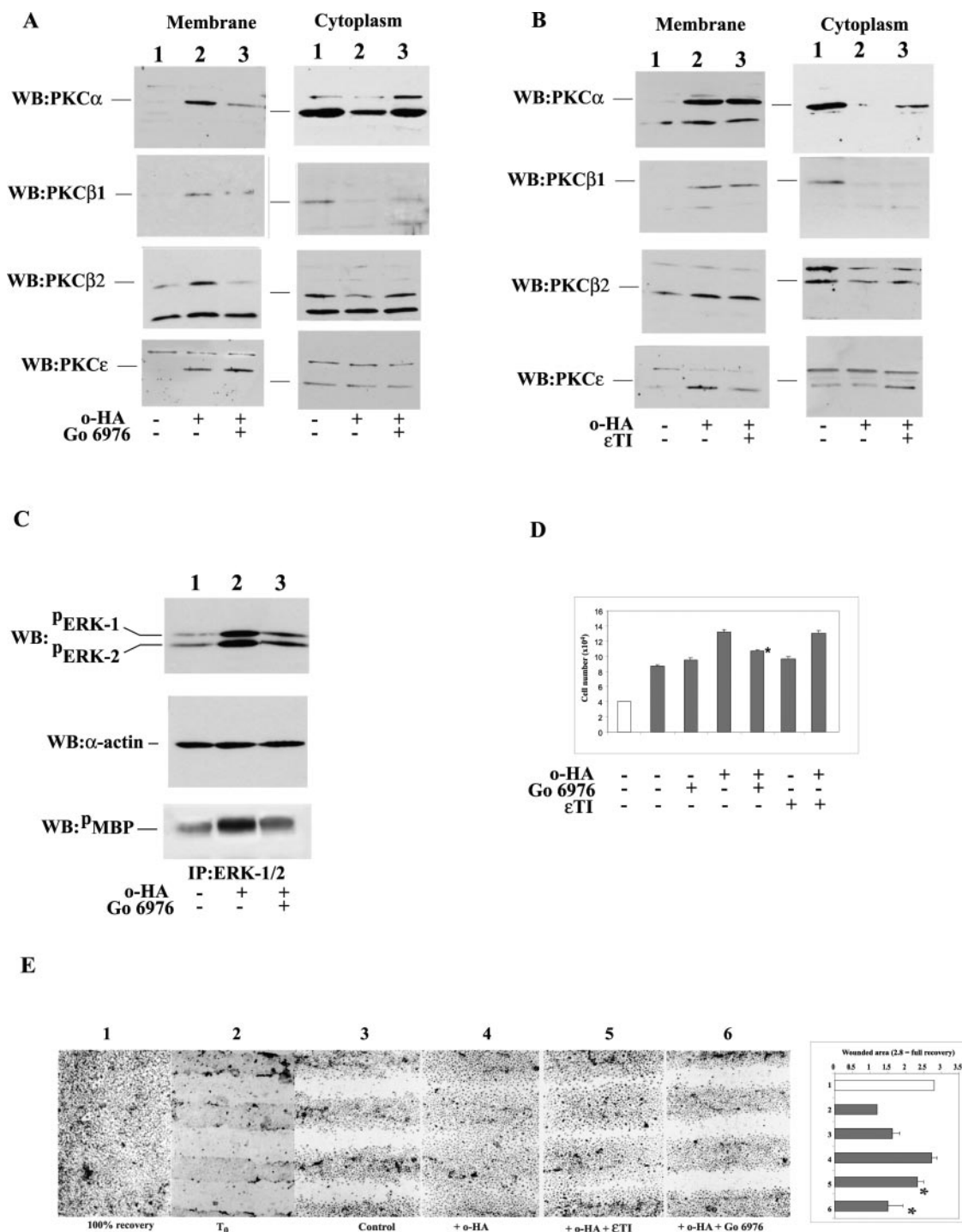


**FIG. 2. Specific isoform inhibitors of PKC affect o-HA-induced signal transduction, mitogenesis, and wound recovery.** *A*, Go 6976 (100 nM), and *B*,  $\epsilon$ TI (20  $\mu$ M) inhibited plasma membrane translocation of PKC $\alpha$ ,  $\beta$ 1,  $\beta$ 2, and  $\epsilon$ , respectively, in o-HA (1  $\mu$ g/ml, 5 min)-treated cells (lane 3). *C*, preincubation with Go 6976 (100 nM/24 h) reduced o-HA (1  $\mu$ g/ml, 5 min)-induced P $^{\text{ERK1/2}}$  expression and activity (lane 3). *D*, Go 6976 (100 nM) significantly inhibited o-HA (1  $\mu$ g/ml)-induced cell proliferation over 72 h. *E*, Go 6976 strongly inhibited o-HA (0.5  $\mu$ g/ml/18 h)-induced wound healing (lane 6, \*,  $p < 0.01$ ), whereas  $\epsilon$ TI had a much weaker, but still significant effect (lane 5, \*,  $p < 0.05$ ). In the bar chart, the first unfilled bar denotes cells with 100% re-growth and the second bar (T<sub>0</sub>) shows totally denuded, freshly wounded cells. All experiments were carried out at least three times and a representative example is shown. WB, Western blot. MBP, myosin basic protein.

arbitrary optical density of 1.0. The intensity of staining between different gels could not be compared because of variation in ECL development time.

## RESULTS

As a continuation of our previous work (31), we studied in detail the up-regulation (between 2 and 10 min) of key signaling proteins and their role in mediating ERK1/2 activation, proliferation, and cell migration (wound recovery).

**Involvement of PLC Isoforms in o-HA Signaling**—Western blot analysis of BAEC extracts showed expression of PLC $\gamma$ 1,  $\beta$ 1,  $\beta$ 2, and  $\delta$ 1 (Fig. 1A). Disappearance of these proteins in antibody mixtures pretreated with specific peptides that blocked the antibody epitope confirmed their identity. Cytoplasm to plasma membrane translocation of PLC isoforms is usually associated with their activation (46, 47). o-HA (1  $\mu$ g/ml)-treated BAEC showed a rapid increase (within 2 min and

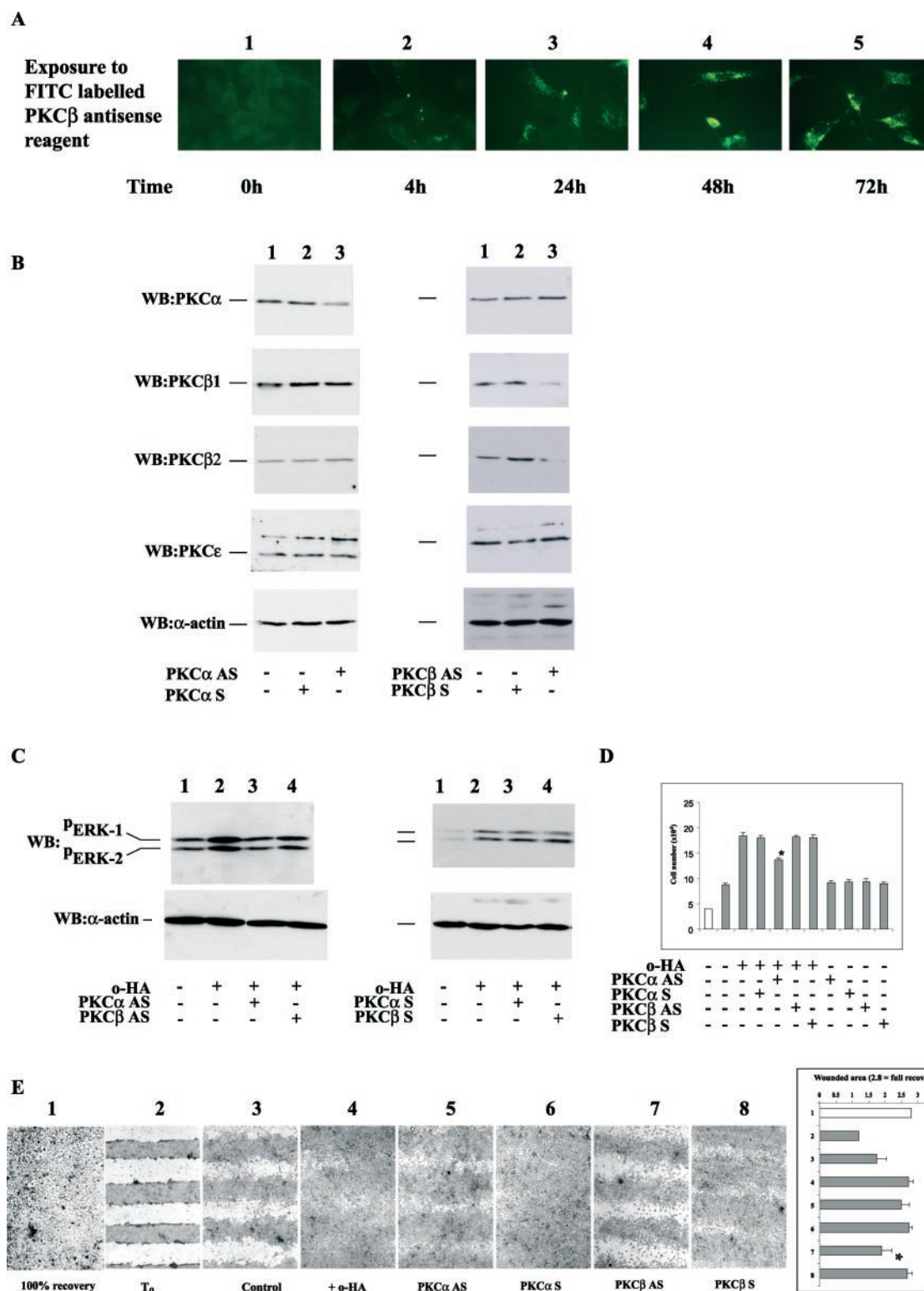


FIG. 3. Effect of antisense reagents on PKC-induced signaling and cell growth. *A*, shows oligonucleotide (*PKCβ* control sequence-FITC) incorporation into BAEC over 0–72 h. Uptake was observed after 24 h (*panel 3*). *B*, BAEC exposed to specific *PKCα* and  $\beta 1/2$  antisense oligonucleotides (*lane 3*) (10  $\mu$ M, 72 h), showed protein down-regulation compared with cells treated with scrambled control oligonucleotides (*lane 2*) and untreated cells (*lane 1*). *C*, after antisense treatment, BAEC were exposed to o-HA (1  $\mu$ g/ml, 5 min). A reduction in pERK1/2 expression was seen in the presence of *PKCα* (*left panel, lane 3*), and to a lesser extent *PKCβ1/2* (*right panel, lane 4*) antisense oligonucleotides. *D*, antisense down-regulation of *PKCα* protein expression significantly reduced o-HA-induced cell proliferation (\*,  $p < 0.05$ ). *E*, *PKCβ1/2* antisense treatment significantly inhibited wound recovery (*lane 7*, \*,  $p < 0.05$ ). In the bar chart, the first unfilled bar denotes cells with 100% re-growth, whereas the second bar ( $T_0$ ), shows freshly wounded, maximally denuded cells. All experiments were repeated at least three times and the figure shows a representative example. WB, Western blot.

maintained after 5 and 10 min) in plasma membrane expression of PLC $\gamma$ 1, and more transiently (maximal after 5 min), in PLC $\beta$ 1 and  $\beta$ 2 (Fig. 1B). An increase in phosphotyrosine stain-

ing (Tyr(P)-99) of anti-PLC $\gamma$ 1 immunoprecipitates also occurred within 2 min of treatment (Fig. 1C). We next examined the involvement of PLC isoforms in ERK1/2 activation. L- $\alpha$ -

Lysophosphatidylcholine-permeabilized BAEC incorporated higher levels of FITC-labeled IgG than nonpermeabilized cells, as shown by fluorescent microscopy and FACS analysis (Fig. 1D, *i* and *ii*, respectively). Degradation of loaded antibodies occurred after about 4 h making this technique unsuitable for long term studies (data not shown). Only anti-PLC $\gamma$ 1 (5  $\mu$ g/ml) reduced the o-HA (1  $\mu$ g/ml, 5 min)-induced  $^3$ P-ERK1/2 formation (74 and 80%) and ERK activity (70%), respectively, compared with IgG control antibodies. (Fig. 1E). These results suggest that o-HA-induced signaling through PLC $\gamma$ 1 may be primarily involved in stimulating mitogenesis.

**Role of PKC Isoforms in o-HA-induced Mediation of ERK1/2 Activation, Mitogenesis, and Wound Recovery in BAEC**—We showed previously that o-HA-induced ERK1/2 activation, and subsequent mitogenesis, were partially dependent on activation and associated plasma membrane translocation of PKC $\alpha$ , - $\beta$ 1, - $\beta$ 2, and - $\epsilon$  (31). Pilot studies based on previous published data (48) showed that Go 6976 (100 nM/24 h preincubation) reduced plasma membrane translocation of PKC $\alpha$ , - $\beta$ 1, and - $\beta$ 2 (84, 73, and 90%, respectively) but not  $\epsilon$  after addition of o-HA (1  $\mu$ g/ml, 5 min). Similarly, the  $\epsilon$ -translocation inhibitor ( $\epsilon$ TI, 20  $\mu$ M/24 h preincubation) attenuated o-HA-induced plasma membrane translocation of PKC $\epsilon$  (71%), but had no effect on PKC $\alpha$ , - $\beta$ 1, or - $\beta$ 2 (Fig. 2, A and B) (49). The inhibitors were not cytotoxic as shown by cell growth assays in SPM and trypan blue exclusion. Only Go 6976 (100 nM/24 h) notably reduced o-HA-induced formation of  $^3$ P-ERK1/2 (75 and 73%, respectively) and ERK activity (78%) compared with untreated cells (Fig. 2C). Pretreatment with Go 6976 significantly inhibited o-HA-induced cell proliferation (70%) compared with untreated cells ( $p < 0.05$ ) although  $\epsilon$ TI had no inhibitory effect (Fig. 2D). Similarly, the presence of Go 6976 almost completely inhibited o-HA-induced wound healing ( $p < 0.001$ ), although  $\epsilon$ TI had a much smaller (18%) but still significant effect ( $p < 0.05$ , Fig. 2E).

To distinguish between the functional importance of PKC $\alpha$  and - $\beta$  isoforms, BAEC were exposed to specific antisense or scrambled oligonucleotides. Fluorescent monitoring of FITC-labeled scrambled PKC $\beta$  showed appreciable cytoplasmic incorporation over 24–72 h (Fig. 3A). Addition of PKC $\alpha$  antisense reagent (10  $\mu$ M) with LipofectAMINE 2000 (10  $\mu$ g/ml), to semi-confluent BAEC, resulted in down-regulation in PKC $\alpha$  protein expression after 72 h (55%) without affecting  $\beta$ 1,  $\beta$ 2, or  $\epsilon$  isoforms, compared with the controls. PKC $\beta$ 1/2 antisense reagent (10  $\mu$ M) produced 70 and 75% reduction in expression of those isoforms, respectively, without affecting PKC $\alpha$  or - $\epsilon$  (Fig. 3B). Antisense inhibition of PKC $\alpha$  reduced  $^3$ P-ERK1/2 expression in o-HA (1  $\mu$ g/ml, 5 min)-treated cells (73 and 72%, respectively), whereas PKC $\beta$  inhibition resulted in a smaller reduction (41 and 37%, respectively) (Fig. 3C). Scrambled oligonucleotides had no effect on  $^3$ P-ERK1/2 expression. Incorporation of PKC $\alpha$  antisense oligonucleotide also significantly reduced o-HA-induced BAEC proliferation by 49% ( $p < 0.05$ , analysis of variance) but only weakly inhibited wound recovery (15%  $p < 0.05$ ) (Fig. 3, D and E, respectively). Treatment with PKC $\beta$  antisense oligonucleotide had no effect on proliferation, but strongly inhibited o-HA-induced wound recovery (85%,  $p < 0.001$ ). In conclusion, the  $\alpha$  isoform may be more important in regulating mitogenesis through ERK1/2, whereas the  $\beta$  isoforms, and to a lesser extent  $\epsilon$ , are primarily involved in cell migration/wound recovery.

**Activation of Ras in o-HA-treated BAEC: Role in Cell Mitogenesis and Wound Healing**—Ras activity increased 5.5-fold within 2 min, and remained higher than control levels 10 min after o-HA treatment (1  $\mu$ g/ml) (Fig. 4A). Analysis of total Ras expression indicated equality of protein loading. Pilot studies

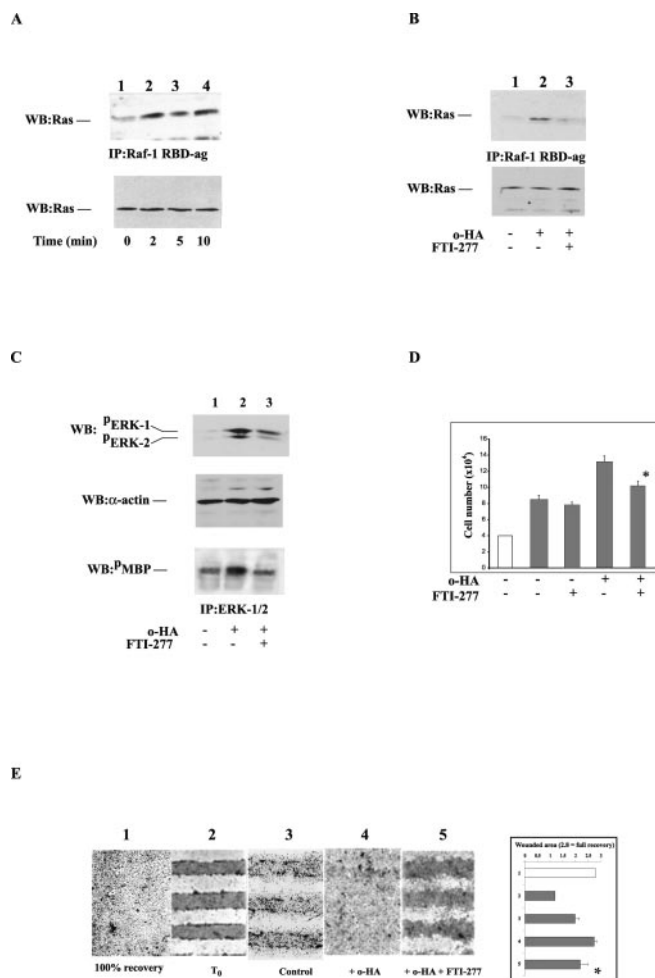


**Fig. 4. Inhibition of o-HA-induced Ras activation by FTI-277 reduces BAEC mitogenesis and wound recovery.** A, BAEC showed an increase in active Ras expression within 2 min of o-HA (1  $\mu$ g/ml) treatment (lanes 2–4). Total Ras expression is shown as a loading control. B, FTI-277 (1  $\mu$ M, 24 h) inhibited o-HA (1  $\mu$ g/ml, 5 min)-induced Ras activation (lane 3). C, o-HA (1  $\mu$ g/ml, 5 min)-induced  $^3$ P-ERK1/2 expression and activity were markedly reduced in FTI-277 (1  $\mu$ M, 24 h)-treated cells (lane 3).  $\alpha$ -Actin loading controls are also shown. D, o-HA (1  $\mu$ g/ml)-induced BAEC proliferation was significantly reduced after 72 h (\*,  $p < 0.05$ ) in the presence of FTI-277 (1  $\mu$ M). E, FTI-277 (1  $\mu$ M, 24 h) significantly inhibited o-HA (0.5  $\mu$ g/ml, 18 h)-induced wound recovery (lane 5, \*,  $p < 0.05$ ). In the bar chart, the first unfilled bar denotes cells with 100% re-growth, whereas the second bar ( $T_0$ ) shows freshly wounded, maximally denuded cells. All experiments were repeated at least three times and shows a representative example. WB, Western blot. MBP, myosin basic protein.

using FTI-277, a potent and specific inhibitor of Ras farnesyl-transferase processing (50), showed an optimum inhibitory concentration that avoided cellular cytotoxicity of 1  $\mu$ M over 24 h. BAEC pretreated with FTI-277 before addition of o-HA (1  $\mu$ g/ml, 5 min) showed a 71% reduction in Ras activity (Fig. 4B), as well as the degree of  $^3$ P-ERK1/2 formation (62 and 74%, respectively) and ERK activity (83%) (Fig. 4C). A significant reduction in both o-HA-induced cell proliferation and wound recovery occurred in the presence of FTI-277 (51%,  $p < 0.05$ , Fig. 4D, and 63%,  $p < 0.05$ , Fig. 4E, respectively). To confirm these findings, Ras protein was down-regulated using specific Ras antisense oligonucleotides. Pilot studies showed exposure of BAEC cultured in SPM to 10  $\mu$ M antisense oligonucleotides with 10  $\mu$ g/ml LipofectAMINE 2000 reduced Ras protein expression by 70% after 72 h compared with sense controls (Fig. 5A). o-HA (1  $\mu$ g/ml, 5 min)-induced activation of Ras, measured in Raf-1 kinase RBD-agarose immunoprecipitates, was reduced

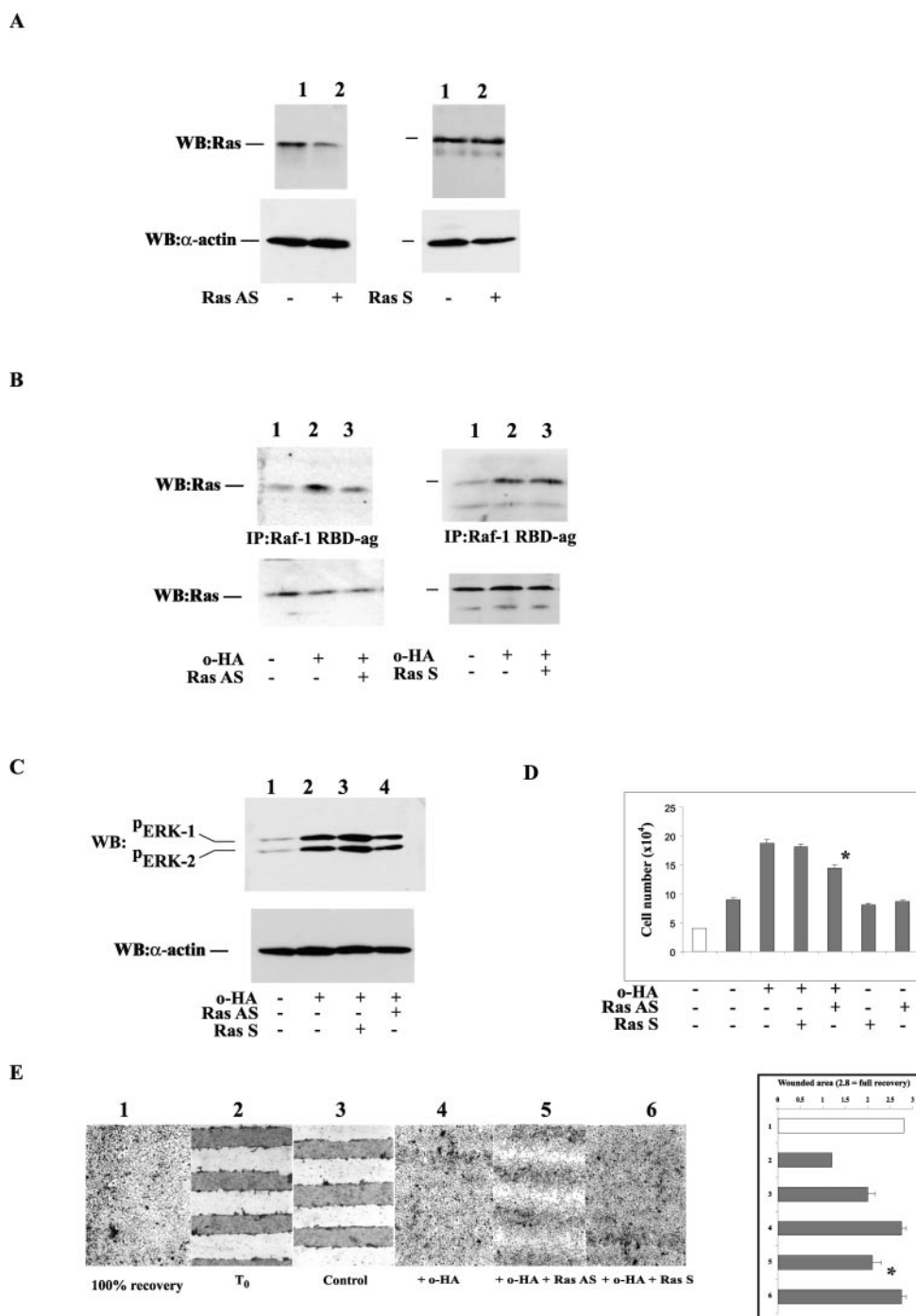


**FIG. 5. Down-regulation of Ras protein using antisense reagents reduces o-HA-induced signal transduction and angiogenesis in BAEC.** *A*, BAEC exposed to *Ras* antisense oligonucleotides (left panel, lane 2, 10  $\mu\text{M}$ , 72 h) showed a reduction in Ras protein expression compared with control sense-treated cells (right panel). *B*, cells stimulated with o-HA (1  $\mu\text{g}/\text{ml}$ , 5 min) after *Ras* antisense treatment showed a reduction in activation of Ras protein (left panel, lane 3).  $\alpha$ -Actin protein loading controls are also shown. *C* shows a reduction in  $^{\text{p}}\text{ERK1/2}$  expression in cells treated as in *B* above (lane 4). *D*, antisense treatment was sufficient to significantly reduce o-HA (1  $\mu\text{g}/\text{ml}$ , 72 h)-induced cell proliferation, and *E*, o-HA (0.5  $\mu\text{g}/\text{ml}$ , 18 h)-induced wound recovery (lane 5) (\*,  $p < 0.05$ , in both cases). In the bar chart (*E*), the first unfilled bar denotes cells with 100% re-growth and the second bar ( $T_0$ ) shows freshly wounded, maximally denuded cells. All experiments were repeated at least three times and shows a representative example. WB, Western blot.

by 72% (Fig. 5B), whereas  $^{\text{p}}\text{ERK1/2}$  formation decreased by 31 and 33%, respectively, in antisense-treated BAEC (Fig. 5C). BAEC cultured with antisense reagent in the presence of o-HA demonstrated a significant reduction in cell proliferation after 72 h (55%,  $p < 0.05$ , Fig. 5D), and wound recovery after 18 h (62%,  $p < 0.05$ , Fig. 5E), compared with sense controls. Neither Go 6976 nor *PKC* antisense reagents notably reduced Ras activity (data not shown), suggesting Ras activation was independent of *PKC*.

*Involvement of G-proteins in o-HA-induced Signal Transduction*—Little is known of the mechanisms through which o-HA receptors initiate second messenger activation. Because we have demonstrated activation of several isoforms of PLC, we examined the involvement of heterotrimeric G-proteins in this process. BAEC expressed the  $G\alpha_{i/o/t/z}$ ,  $G\beta$  subunit (after o-HA treatment 1  $\mu\text{g}/\text{ml}$ , 5 min),  $G\alpha_{s/olf}$  and  $G\alpha_{q/11}$  subtypes (Fig. 6A). Antibodies treated with peptide inhibitors (+) served as negative controls to confirm expression of the protein and specificity

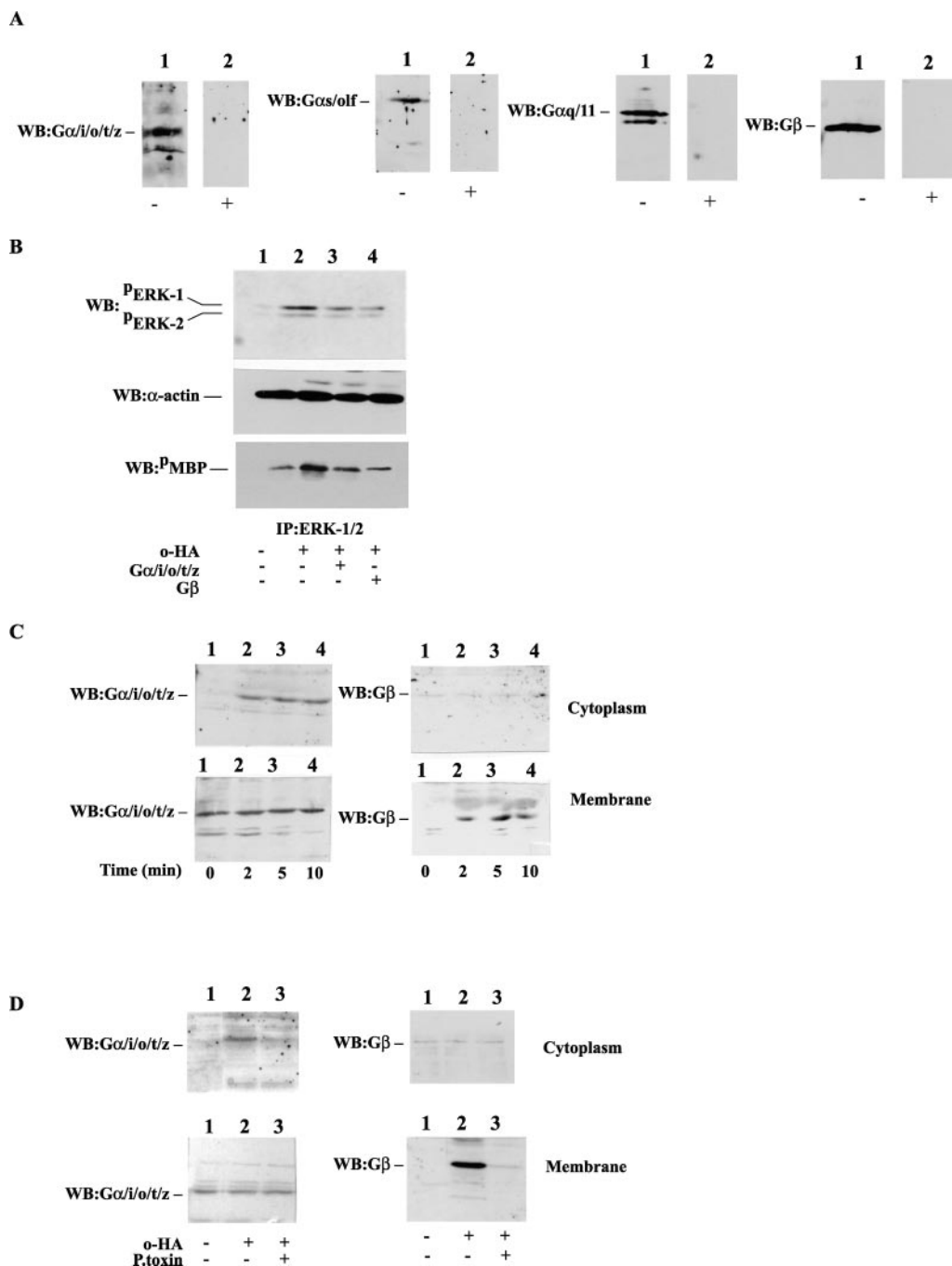


**FIG. 6. o-HA induces activation of pertussis toxin-sensitive G-proteins in BAEC.** A, expression of  $G_{\alpha_{i/o/t/z}}$ ,  $G_{\alpha_{s/olf}}$ ,  $G_{\alpha_{q/11}}$ , and  $G_{\beta}$  subunits (after o-HA treatment 1  $\mu\text{g/ml}$ , 5 min) in BAEC was demonstrated by Western blotting (WB). Confirmation of specificity is shown by the disappearance of the protein band in specific inhibitory peptide-treated antibody mixtures (shown as +, lane 2). B, cell cytoplasm loading of antibodies to either  $G_{\alpha_{i/o/t/z}}$  (lane 3) or  $G_{\beta}$  subunits (lane 4) inhibited o-HA-induced  $^{\text{P}}\text{ERK1/2}$  expression and ERK activity. C shows appearance of  $G_{\beta}$  subunits in the membrane fraction (right panel) and  $G_{\alpha_{i/o/t/z}}$  in the cytoplasmic fraction (left panel) within 2 min in o-HA (1  $\mu\text{g/ml}$ )-treated cells (lanes 2–4). D, preincubation of cells with pertussis toxin (*P.toxin*) (100 ng/ml, 6 h) inhibited o-HA-induced (1  $\mu\text{g/ml}$ , 5 min) redistribution and separation of G-proteins (lane 3). All experiments were repeated at least three times and a representative example is shown. MBP, myosin basic protein.

of the antibodies. Cytoplasmic loading of either anti- $G_{\alpha_{i/o/t/z}}$  or anti- $G_{\beta}$  (5  $\mu\text{g/ml}$  as described earlier) inhibited o-HA (1  $\mu\text{g/ml}$ , 5 min)-induced  $^{\text{P}}\text{ERK1/2}$  expression (66 and 62% and 74 and 68%, respectively) and ERK activity by 70 and 75%, respectively (Fig. 6B), whereas anti- $G_{\alpha_{s/olf}}$  and  $G_{\alpha_{q/11}}$  had no inhibitory effect. Activation of  $G_{\alpha}$  proteins causes their translocation from the plasma membrane to the cytoplasm together with formation of both  $G_{\alpha}$  and  $G_{\beta\gamma}$  subunits, the  $G_{\beta\gamma}$  subunits remaining plasma membrane-bound (51).  $G_{\alpha_{i/o/t/z}}$  proteins were detected in the cytoplasmic fraction and  $G_{\beta}$  subunits in

the membrane fraction, within 2 min, in o-HA (1  $\mu\text{g/ml}$ )-treated BAEC (Fig. 6C). Pretreatment of BAEC with the specific  $G_{\alpha_{i/o}}$  protein inhibitor pertussis toxin (52) (100 ng/ml, 6 h), reduced o-HA (1  $\mu\text{g/ml}$ , 5 min) induced cytoplasmic expression of  $G_{\alpha_{i/o/t/z}}$  proteins by 65%, and appearance of  $G_{\beta}$  subunits in the membrane fraction by  $\sim 95\%$  (Fig. 6D). No cellular cytotoxicity was found at this concentration. Pretreatment of BAEC with pertussis toxin markedly reduced o-HA (1  $\mu\text{g/ml}$ , 5 min) induced PKC $\alpha$ , - $\beta 1$ , and - $\beta 2$  membrane translocation (92, 55, and 77%, respectively, Fig. 7A),  $^{\text{P}}\text{ERK1/2}$  expression (50 and

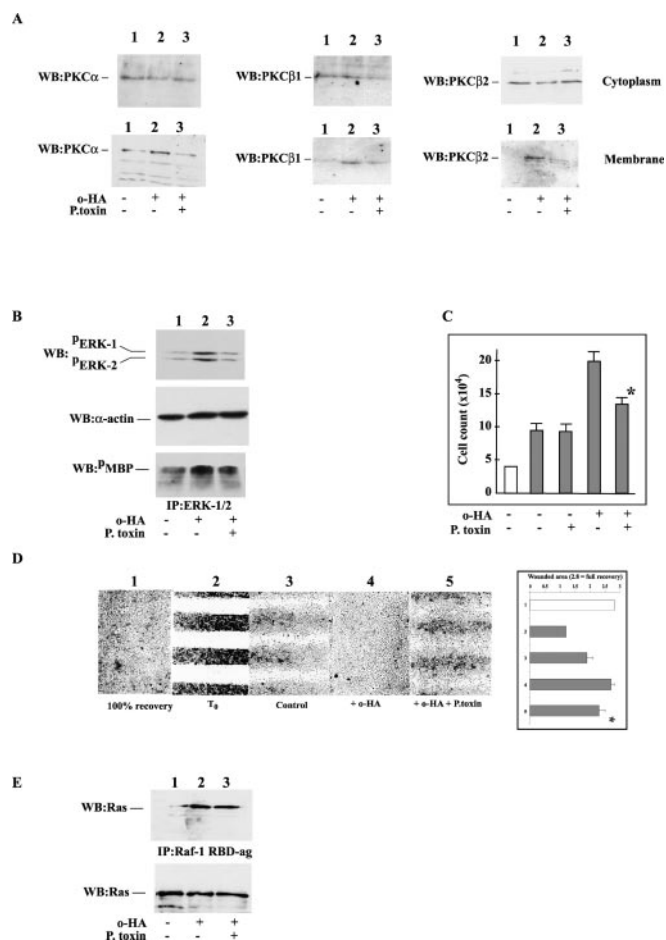


**FIG. 7. Pertussis toxin inhibits o-HA-induced signal transduction and mitogenesis.** A, BAEC pretreated with pertussis toxin (*P. toxin*) (100 ng/ml, 6 h) reduced plasma membrane translocation of PKC $\alpha$ ,  $\beta$ 1, and  $\beta$ 2 isoforms in the presence of o-HA (1  $\mu$ g/ml, 5 min) (lane 3). B, pretreatment of BAEC with pertussis toxin also inhibited o-HA-induced <sup>32</sup>P-ERK1/2 expression and ERK activity (lane 3), as well as, C, cell proliferation after 72 h (\*,  $p < 0.05$ ). D, o-HA (0.5  $\mu$ g/ml, 18 h)-induced wound recovery was significantly reduced in the presence of the toxin (lane 5, \*,  $p < 0.05$ ). In the bar chart, the first unfilled bar denotes cells with 100% re-growth, and the second bar ( $T_0$ ) shows freshly wounded maximally denuded cells. E, shows the inability of pertussis toxin to inhibit Ras activity in o-HA (1  $\mu$ g/ml, 5 min)-treated cell lysates processed as described previously (lane 3). All experiments were repeated at least three times and the above shows a representative example. WB, Western blot. MBP, myosin basic protein.

55%, respectively) and activity (51%) (Fig. 7B). Pertussis toxin at the same concentration significantly inhibited both proliferation (72 h) and wound recovery (18 h) of BAEC (66%,  $p < 0.05$ , Fig. 7C and 47%,  $p < 0.05$ , Fig. 7D, respectively), compared with vehicle-only treated cells. o-HA-induced Ras activation was not affected in pertussis toxin-treated cells (Fig. 7E), suggesting it acts on a separate pathway. When the previous experiments were repeated using the specific G $\alpha_q$  inhibitor GP ant-2A (53), there was no demonstrable effect on o-HA-induced mitogenic or wound healing responses (data not shown). These results suggest that activation of G $\alpha_{i/o}$  proteins in o-HA-treated BAEC is at least in part responsible for control of tyrosine kinase-associated events resulting in mitogenesis and wound healing. We next performed co-precipitation studies to identify possible binding partners for G $\alpha_{i/o}$  proteins and G $\beta(\gamma)$  subunits. There was no association between G $\alpha_{i/o/t/z}$  and G $\beta$  subunit immunoprecipitates from o-HA (1  $\mu$ g/ml, 2, 5, and 10 min)-treated cells, and PLC $\beta$ 1,  $\beta$ 2, or  $\beta$ 3 (data not shown). However, G $\beta$  subunits co-precipitated with PLC $\gamma$ 1 within 2 min (Fig. 8A), and this was reduced by 80% after preincubation of

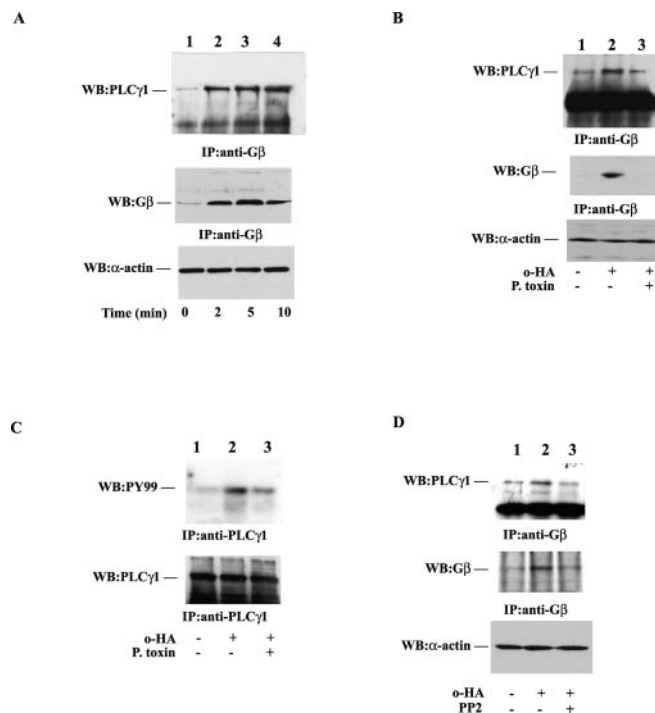


**FIG. 8. G $\beta$  subunits co-precipitate with PLC $\gamma$ : sensitivity to both pertussis toxin and PP2.** A, immunoprecipitated G $\beta$  subunits co-precipitated with PLC $\gamma$ 1 within 2 min of o-HA (1  $\mu$ g/ml) treatment (lanes 2–4). B, preincubation of BAEC with pertussis toxin (*P. toxin*) (100 ng/ml, 6 h) reduced o-HA (1  $\mu$ g/ml, 5 min)-induced association of G $\beta$  subunits with PLC $\gamma$ 1 in G $\beta$  immunoprecipitates (lane 3). C, the same treatment also reduced o-HA (1  $\mu$ g/ml, 5 min)-induced phosphorylation of PLC $\gamma$ 1 (lane 3). D, preincubation of cells with PP2 (100 nM/24 h) also inhibited o-HA (1  $\mu$ g/ml, 5 min)-induced G $\beta$  subunit co-precipitation with PLC $\gamma$ 1 (lane 3), measured in G $\beta$  immunoprecipitated cell lysates. All experiments were repeated at least three times and the above shows a representative example. WB, Western blot.

BAEC with pertussis toxin (Fig. 8B). Tyrosine phosphorylation of PLC $\gamma$ 1 was also partially inhibited by 64% following preincubation with pertussis toxin in o-HA-treated cells (Fig. 8C). Finally, preincubation with the Src kinase inhibitor PP2 (100 nM, 24 h), reduced PLC $\gamma$ 1 association with G $\beta$  subunits (90%) in G $\beta$  immunoprecipitates (Fig. 8D). These results suggest a role for G protein regulation independent of Ras in a distinct signal transduction pathway.

**o-HA Activates Ras via Src and Subsequent Mobilization of Shc in BAEC**—Previous work has demonstrated that both recruitment to and interaction of Src with CD44 following HA binding promoted cell migration in human ovarian tumor cells (SK-OV-3 ipc) (54). Activation of Src is one mechanism through which the adapter protein Shc can stimulate Ras. Specificity of Src antibodies was determined by comparison with staining in a control whole cell lysate (WEHI-231, Fig. 9A). Activation (within 5 min) and tyrosine phosphorylation (within 2 min) of Src lasted up to 10 min in o-HA (1  $\mu$ g/ml)-treated BAEC (Fig. 9B). The Src family kinase inhibitor PP2, used at the optimum inhibitory concentration of 100 nM/24 h (determined from pilot studies), reduced tyrosine phosphorylation and activation of Src in o-HA (1  $\mu$ g/ml, 5 min)-treated BAEC (68 and 88%, respectively, Fig. 9C). Pretreatment of BAEC with pertussis toxin had no effect (Fig. 9D), suggesting that upstream activating components may not include heterotrimeric G proteins.

Preincubation of BAEC with PP2 before addition of o-HA (1 and 0.5  $\mu$ g/ml, respectively), resulted in a significant decrease in cell proliferation after 72 h (65%,  $p < 0.05$ , Fig. 10A), and wound recovery after 18 h treatment (82%,  $p < 0.05$ , Fig. 10B). PP2 also inhibited activation of Ras (53%, Fig. 10C), <sup>32</sup>P-ERK1/2

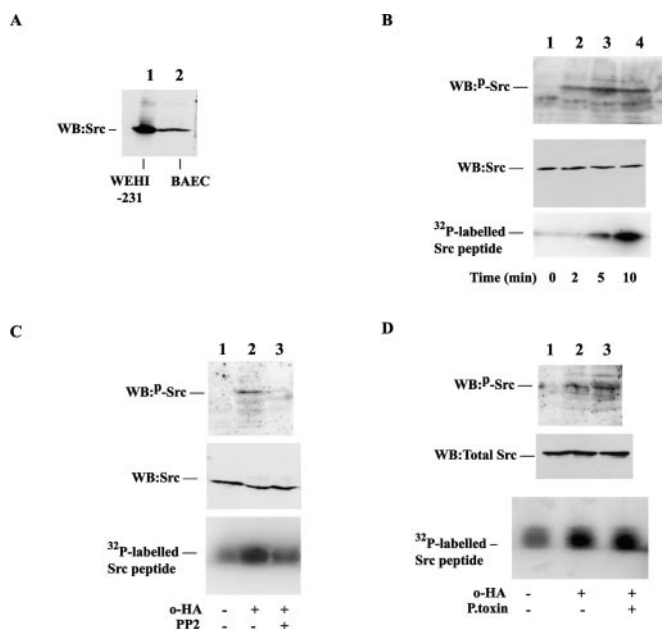


**FIG. 9. o-HA induces activation of Src family kinase which is sensitive to PP2.** A shows expression of the Src family kinase in BAEC (lane 2), compared with a positive control cell lysate (lane 1). B, o-HA (1  $\mu$ g/ml)-induced phosphorylation and activation of Src within 5 min of treatment (lanes 2–4). Total Src expression is shown as a loading control. C shows PP2 (100 nM, 24 h) inhibition of o-HA (1  $\mu$ g/ml, 5 min)-induced activation and tyrosine phosphorylation of Src (lane 3). E shows that preincubation of BAEC with pertussis toxin (*P. toxin*) (100 ng/ml, 6 h) had no effect on o-HA (1  $\mu$ g/ml, 10 min)-induced Src activation or tyrosine phosphorylation of proteins (lane 3). All experiments were repeated at least three times and shows a representative example. WB, Western blot.

formation (70 and 56%, respectively), and ERK activity (82%, Fig. 10D), suggesting that it could be an essential upstream component. We attempted to identify the mechanism through which c-Src induced activation of Ras. Ras activation commonly occurs following Shc-Sos-Grb2 complex formation, after autophosphorylation of tyrosine kinase receptors and subsequent dimerization (55). Shc tyrosine phosphorylation may also be dependent on Src (54). BAEC expressed both the p60 and p66 isoforms of Shc, with specificity being determined by peptide inhibition studies (Fig. 11A). Anti-Shc immunoprecipitates from o-HA (1  $\mu$ g/ml)-treated cells showed an increase in tyrosine phosphorylation of both p60 and p66 isoforms within 2 min (Fig. 11B), which was reduced by 65% following preincubation of cells with PP2 (Fig. 11C). Shc co-precipitated with Src within 2 min of o-HA (1  $\mu$ g/ml) treatment (Fig. 11D), and this was reduced in the presence of PP2 (91 and 72% respectively, Fig. 11E). Shc did not co-precipitate with heterotrimeric G proteins, G $\beta$  subunits, or PLC $\gamma$ 1 (data not included).

Many receptors activate the Ras-MAP kinase pathway following redistribution and phosphorylation of the adapter protein Shc and its subsequent association with the Sos-Grb2 complex (55). BAEC expressed Sos2 (p170), specificity of the antibody being confirmed using inhibitory peptides (Fig. 11F). Co-precipitation studies showed o-HA-induced association of Sos2 with Shc after 2 min of treatment (Fig. 11G).

#### DISCUSSION

Knowledge of the mechanisms through which HA stimulates angiogenesis will help understand its central role in tissue remodeling and the pathobiology of diseases such as rheumatoid arthritis, diabetic retinopathy, psoriasis, neoplasia, and stroke. We have previously shown that o-HA-stimulated second messenger activity in BAEC involved PKC and MAP kinase (ERK1/2), and resulted in mitogenesis (31). Native, high mo-

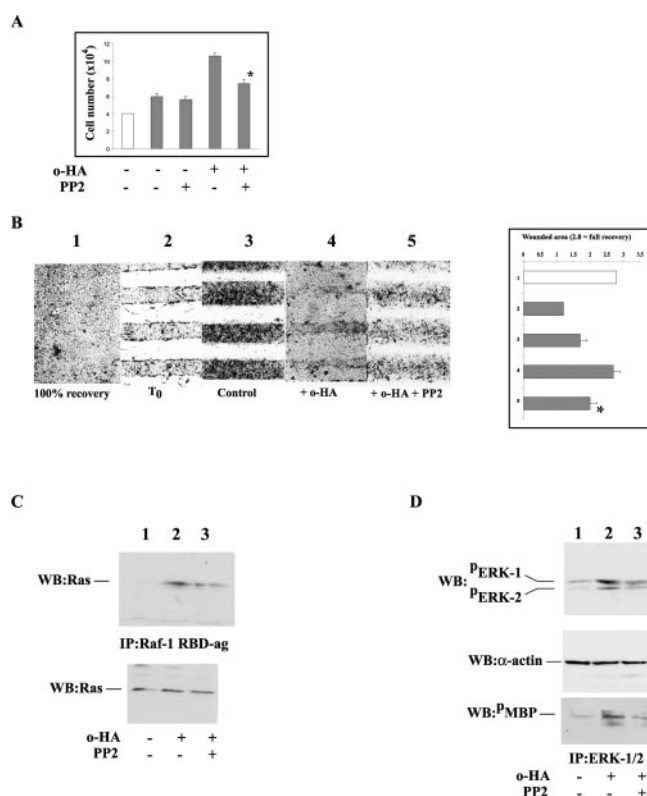


**FIG. 10. PP2 inhibits o-HA-induced signal transduction and mitogenesis in BAEC.** A, PP2 (100 nM, 24 h) significantly inhibited o-HA (1  $\mu$ g/ml)-induced cell proliferation after 72 h (\*,  $p < 0.05$ ). B, PP2 (100 nM for 24 h) significantly inhibited o-HA (0.5  $\mu$ g/ml, 18 h)-induced wound recovery (lane 5, \*,  $p < 0.05$ ). In the bar chart, the first unfilled bar denotes cells with 100% re-growth and the second bar ( $T_0$ ) shows freshly wounded maximally denuded cells. C, PP2 at the same concentration inhibited by o-HA (1  $\mu$ g/ml, 5 min)-induced Ras activation (lane 3), as well as D,  $^3$ P-ERK1/2 formation and ERK activity (lane 3). All experiments were repeated at least three times and shows a representative example. WB, Western blot. MBP, myosin basic protein.

lecular weight HA that is anti-angiogenic *in vivo* had no effect on signal transduction activity, proliferation, or wound recovery in these cells, but inhibited activation by o-HA (3, 11, 35), making BAEC an appropriate and relevant model for the study of the action of o-HA on vascular EC. In this study we show rapid o-HA-induced phosphorylation and membrane translocation of PLC $\gamma$ 1, which is the natural activator of PKC (56). Cytoplasmic incorporation of anti-PLC $\gamma$ 1 antibodies resulted in a notable reduction in ERK1/2 activation, suggesting a role for PLC $\gamma$ 1 in regulation of mitogenesis. PLC  $\beta$ 1 and  $\beta$ 2 isoforms, although transiently translocated, had no effect on ERK1/2 activity. Other studies have shown that mobilization of PLC isoforms could be associated with heterotrimeric G-protein involvement in the signaling process (57).

Cytoplasmic introduction of inhibitory antibodies to either G $\alpha_{s/olf}$  or G $\alpha_{q/11}$  had no effect on o-HA-induced ERK1/2 activity, suggesting that adenyl cyclase-associated and pertussis toxin-insensitive pathways were not involved (57). Furthermore, although the specific G $\alpha_{q/11}$  enzyme inhibitor, GP ant-2A (53), attenuated bombesin-induced  $^3$ P-ERK1/2 expression in our cell system, it had no effect on o-HA-induced signaling or mitogenesis.<sup>2</sup> We found a rapid increase in expression of G $\beta$  subunits in the plasma membrane and G $\alpha_{i/o/t/z}$  in the cytoplasmic fraction of o-HA-treated cells. Cytoplasmic introduction of antibodies to either of these proteins reduced ERK1/2 activity, suggesting the involvement of pertussis toxin-sensitive G-proteins. Formation of G $\beta\gamma$  subunits as well as their cell compartmentalization is a feature of their activation (50), and can result in

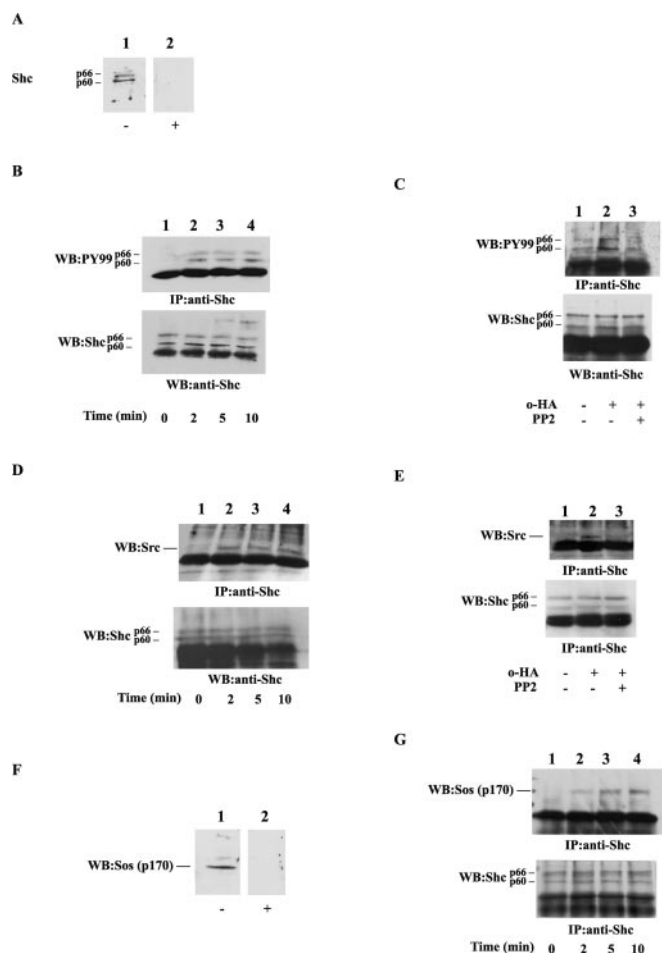


**FIG. 11. o-HA induces Src-dependent mobilization of Shc and its association with Sos.** *A*, expression of Shc (p60/p66) is shown in BAEC lysates, with (+, lane 2) or without (-, lane 1) specific inhibitory antibody blocking peptide. *B*, tyrosine phosphorylation of Shc was increased within 2 min treatment with o-HA (1  $\mu$ g/ml) in Shc immunoprecipitates (lanes 2–4). *C*, PP2 (100 nM, 24 h) reduced o-HA (1  $\mu$ g/ml, 5 min)-induced Shc tyrosine phosphorylation (lane 3). *D*, shows co-precipitation of Src within 2 min of treatment with o-HA (1  $\mu$ g/ml) following Western blotting of Shc immunoprecipitates (lanes 2–4). *E*, o-HA (1  $\mu$ g/ml, 5 min)-mediated co-precipitation of Src with Shc was inhibited in the presence of PP2 (100 nM/24 h) (lane 3). *F*, expression of Sos 2 (p170) in BAEC lysates. Specificity of the antibody was shown following disappearance of the band after treatment with epitope binding inhibitory peptide (+, lane 2). *G*, co-precipitation of Shc with Sos 2 occurred within 2 min of o-HA treatment in Sos immunoprecipitates (lanes 2–4). All experiments were carried out at least three times and a representative example is shown.

complex formation and activation of multiple isoforms of PLC (57). Other studies have shown the ability of G $\beta$  $\gamma$  dimers to activate phosphoinositol-3-kinase resulting in cell proliferation and survival, usually involving activation of the transcription factor NF- $\kappa$ B (58, 59). Although HA fragments can also activate NF- $\kappa$ B in some human carcinoma cell lines (30), our unpublished data<sup>2</sup> showed that phosphoinositol-3-kinase was not activated by o-HA in BAEC, and furthermore, that wortmannin, a specific inhibitor of phosphoinositol-3-kinase (60), had no effect on o-HA-induced signaling events. We demonstrated co-precipitation of G $\beta$  subunits with PLC $\gamma$ 1 after o-HA treatment, and also that inhibition of G $\alpha_{i/o}$  proteins using pertussis toxin was sufficient to inhibit phosphorylation of PLC $\gamma$ 1, plasma membrane translocation of PKC isoforms, and ERK1/2 activity. Cell proliferation and wound recovery were also attenuated suggesting that the association of G $\beta$  with PLC $\gamma$ 1 has an important role in o-HA-induced cell signaling. Other studies have described an association between PLC $\gamma$ 1 and G $\alpha_i$  proteins in

BAEC resulting in PLC $\gamma$ 1 activation (61). This association usually occurred in the presence of another tyrosine kinase-activated co-precipitant such as Src kinase. For example, in human embryonic intestinal epithelial cells, leukotriene D<sub>4</sub> induced co-precipitation of G $\beta$  $\gamma$  subunits with PLC $\gamma$ . This interaction was blocked by PP2, suggesting that physical association of Src with PLC $\gamma$  after agonist stimulation could result in PLC $\gamma$ -G $\beta$  $\gamma$  complex formation (62). Similarly, agonist activation of Src kinase in a variety of cell lines was sensitive to pertussis toxin indicating a role for G $\alpha_i$ -coupled receptors (63). In this study, we showed a rapid increase in tyrosine phosphorylation (within 2 min), and activation (within 5 min) of the Src family kinase in o-HA-treated cells. The importance of Src activation was demonstrated by a significant reduction in o-HA-induced proliferation and wound recovery in PP2-treated cells, whereas preincubation with PP2 reduced o-HA-induced G $\beta$ -PLC $\gamma$ 1 complex formation, suggesting that Src might be a necessary component of PLC $\gamma$ 1 activation. We could not, however, show direct association of Src with PLC $\gamma$ 1. Furthermore, pertussis toxin did not inhibit activation of Src, suggesting its activation was independent of heterotrimeric G-proteins.

Inhibition of ERK1/2 activity by PP2 prompted us to investigate possible downstream signaling intermediates. Ras is a key enzyme necessary for activation of the Raf-1 kinase-Mek-MAP kinase pathway in response to a variety of ligand-receptor interactions, resulting in mitogenesis and oncogenesis (64). Activation of Ras by native HA in rat embryonic fibroblasts (3Y1) (29), and by o-HA in a CD44- and PKC $\zeta$ -dependent manner in human T24 bladder carcinoma cells, has previously been demonstrated (30). We show an o-HA-induced increase in Ras activity within 2 min, whereas ERK1/2 activity, cell proliferation, and wound recovery were inhibited by the Ras farnesyl-transferase inhibitor FTI-277 and Ras antisense reagent. Activation of Ras was independent of heterotrimeric G proteins and PKC, because neither pertussis toxin nor Go 6976 were inhibitory. Also, the direct PKC activator phorbol 12,13-dibutyrate was unable to activate Ras.<sup>2</sup>

Conventional growth factor receptor activation of Ras involves phosphotyrosine-dependent association of Shc with an autophosphorylated receptor (51). The subsequent interaction between phosphorylated Shc and the adapter protein Grb2 causes membrane translocation of the Grb2:Sos complex where Sos mediates guanine nucleotide exchange on Ras (65). Release of G $\beta$  $\gamma$  subunits from pertussis toxin-sensitive heterotrimeric G-proteins can also result in tyrosine phosphorylation of Shc and induction of Grb2:Sos complex formation (52) or Shc-Grb2:Src complex formation (57). In this study, Shc became tyrosine phosphorylated within 2 min of treatment with o-HA, and furthermore, co-precipitated strongly with Src. PP2 treatment was sufficient to reduce Shc tyrosine phosphorylation, complex formation between Src and Shc, and subsequent Ras activity. Finally, we demonstrated co-precipitation of Shc with Sos, suggesting that o-HA activates Ras through Src-dependent activation of Shc-Grb2-Sos. This mechanism of Ras activation has previously been described following treatment of human epidermoid carcinoma cells (A431) with (*S*)-12-hydroxyeicosatetraenoic acid (54).

Elsewhere, we have shown that plasma membrane translocation and activation of PKC $\alpha$ ,  $\beta$ 1,  $\beta$ 2, and  $\epsilon$  were important in formation of pERK1/2 and cell mitogenesis (31). We have examined the function of these isoforms in more detail. Activation of ERK1/2 and mitogenesis occurred mainly through PKC $\alpha$ , whereas PKC $\beta$ 1/2 had a much weaker effect but was necessary for efficient wound recovery in o-HA-treated cells. Other authors have highlighted the importance of PKC $\alpha$  in mediating cell proliferation induced by phorbol esters in rat microvessel

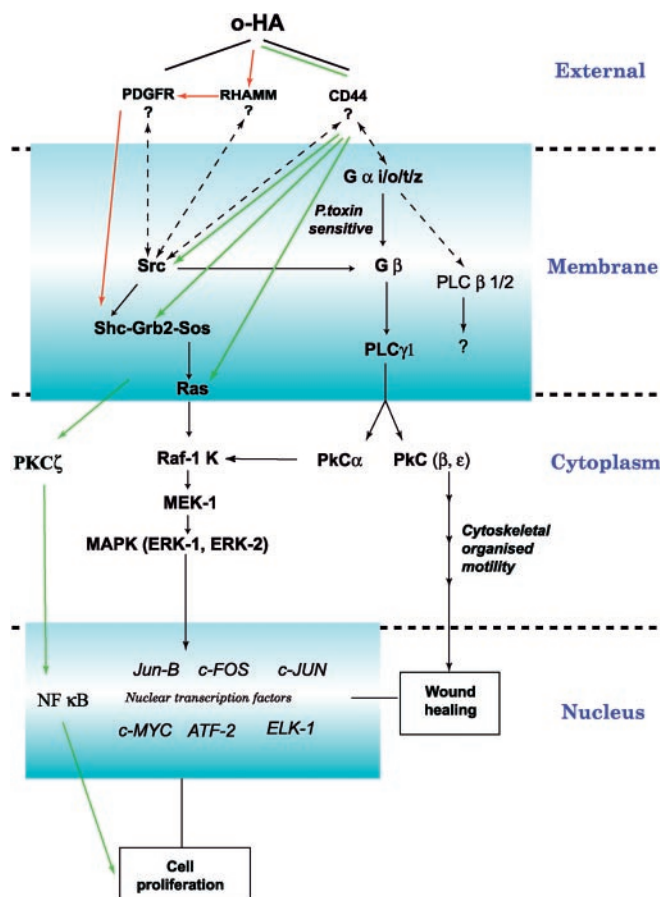


FIG. 12. Schematic diagram showing the signal transduction pathways through which o-HA induces vascular endothelial cell mitogenesis and wound recovery. Previous work has shown the ability of o-HA to induce vascular EC proliferation through the CD44 receptor (78). Similarly, signaling through RHAMM can also activate proliferation via ERK activation (33). In depth examination of signaling intermediates has not been studied. We show that o-HA induces mobilization of  $G_{\alpha i/o/t/z}$  resulting in  $G_{\beta}$ -dependent activation of  $PLC_{\gamma 1}$ .  $PKC_{\alpha}$  induced mitogenesis through ERK1/2 nuclear translocation and activation of early response genes. Activation of  $PKC_{\beta}$  and to a lesser extent  $PKC_{\epsilon}$  was important for wound recovery. o-HA also activated Src family kinase, which bound to Shc and activated Ras following Shc-Grb2-Sos complex formation. This pathway was important for both wound healing and proliferation.  $G_{\beta}$ - $PLC_{\gamma 1}$  complex formation was also dependent on Src suggesting an important interaction between these two pathways. In other cell types, HA binding to CD44 results in association and activation of c-Src, Ras, and Grb2 resulting in cell activation (30, 54, 66) (highlighted in green), similarly RHAMM can initiate proliferation via activation of the platelet-derived growth factor receptor and ERK (75) (highlighted in red). Our findings suggest that a similar pattern of receptor-second messenger interaction may occur in BAEC. In conclusion, our work demonstrates the possibility that more than one receptor can modulate o-HA-induced angiogenesis in BAEC. The precise interactions between o-HA receptors and second messengers should be the focus of further study. Dotted lines represent possible interactions between primary second messengers and o-HA receptors, whereas multiple arrowheads indicate the likely presence of unidentified intermediates.

EC (67), and in vascular endothelial growth factor-treated human umbilical vein EC (68). Similarly, a role for  $PKC_{\beta}$  in regulation of cell migration, in human coronary smooth muscle cells induced by high glucose (69), and in porcine vascular smooth muscle cells treated with insulin-like growth factor (70), has been described. Promotion of cell movement through activation of  $PKC_{\beta}$  may involve its localization to specific microtubule-organizing centers and microtubules in the cytoskeleton (71). HA-induced motility of Ras-transformed 10T1/2 (C3) fibroblasts in a  $PKC$ -dependent manner that was also associated with rapid uptake of HA by both CD44 and RHAMM

receptors (72). Our own data<sup>2</sup> has shown that inhibitors of tyrosine phosphorylation (genistein) and Mek-1 (PD98059) were sufficient to reduce wound recovery, suggesting these signaling pathways are also important.

Here we have described for the first time, the signaling mechanisms through which o-HA stimulates angiogenesis in vascular EC (see Fig. 12). At least two distinct pathways converge upstream of the MAP kinase resulting in cell activation. Heterotrimeric G-proteins and in particular, release of  $G_{\beta}(\gamma)$  subunits seem to be important in mediating  $PLC_{\gamma 1}$  activation of  $PKC$ , whereas separately, Src family kinases activate Ras through Shc-Grb2-Sos complex formation. The pathways may overlap because PP2 inhibited  $G_{\beta}$  association with  $PLC_{\gamma 1}$ . Identification of the interactions between HA receptors and their primary second messengers should be the focus of further studies. More than one potentially important HA cell surface receptor has been described in vascular EC. We have previously shown expression of the CD44 receptor in BAEC and its role in promotion of o-HA-induced tyrosine phosphorylation (31). Other studies have reported a similar response to o-HA in human glioma cells (73), whereas association of CD44 with Src was shown in human neutrophils (74) and human ovarian tumor cells (53) after treatment with o-HA. Expression of RHAMM was demonstrated on the cell surface of a variety of primary human vascular EC (33). Both native HA and in particular o-HA treatment, resulted in RHAMM-dependent tyrosine phosphorylation and MAP kinase activation, suggesting that this was the functional HA receptor. Src activity has also been associated with RHAMM-mediated cell motility in mouse fibroblasts (26). Other EC-specific receptors such as white fat-HA binding protein, detected in human aorta and atherectomy samples (76), have also been identified, although their importance in mediation of HA-induced signal transduction has not been determined. Our results leave open the possibility that more than one o-HA-specific receptor may be present on the surface of BAEC. The mechanism through which o-HA (F3 fragments) binds to receptors and activates angiogenesis in both our *in vivo* and *in vitro* models should be examined in detail. Whereas other authors have demonstrated the ability of native HA to weakly activate signal transduction activity associated with proliferation in vascular EC of different origin (33), different sized fragments of HA may elicit specific responses in individual cells for a variety of reasons. For instance, it may depend on the types of receptor expressed, the operational signal transduction pathways available (which may work in synergy as described in this work), and also on the ability of the molecule to specifically interact with the appropriate link module binding site on the receptor (77). The data presented here may be useful in the identification of potential targets for modulation of angiogenesis in a variety of diseases associated with abnormal EC growth.

**Acknowledgment**—We thank Mick Hoult for help in preparation of the figures.

#### REFERENCES

- Martin, J. F., and Hassall, D. G. (1990) in *The Endothelium: An Introduction to Current Research* (Warren, J. B., ed) pp. 95–105, Wiley-Liss Inc., New York
- Folkman, J. (1995) *Nat. Med.* **1**, 27–31
- Krupinski, J., Kaluza, J., Kumar, P., Kumar, S., and Wang, J. M. (1994) *Stroke* **25**, 1794–1798
- Brink, J., and Heldin, P. (1999) *Exp. Cell Res.* **252**, 342–351
- Scott, J. E. (1995) *J. Anat.* **187**, 259–269
- West, D. C., and Kumar, S. (1989) *Ciba Found. Symp.* **143**, 187–207
- West, D. C., and Kumar, S. (1988) *Lancet* **1**, 715–716
- West, D. C., and Kumar, S. (1991) *Int. J. Radiol.* **61–62**, 55–60
- Watanabe, M., Nakayasu, K., and Okisaki, S. (1993) *Nippon Ganka Gakkai Zasshi* **97**, 1034–1039
- West, D. C., and Kumar, S. (1989) *Exp. Cell Res.* **183**, 176–196
- Deed, R., Rooney, P., Norton, J. D., Freemont, A. J., and Kumar, S. (1997) *Int. J. Cancer.* **71**, 116–122

12. Sattar, A., Rooney, P., Kumar, S., Pye, D., West, D. C., Scott, I., and Ledger, P. (1994) *J. Invest. Dermatol.* **103**, 576–579
13. Montesano, R., Kumar, S., Orci, L., and Pepper, M. S. (1996) *Lab. Invest.* **75**, 249–262
14. West, D. C., Hampson, I. N., Arnold, F., and Kumar, S. (1985) *Science* **228**, 1324–1327
15. Kumar, S., Ponting, J., Rooney, P., Kumar, P., Pye, D., and Wang, M. (1994) in *Angiogenesis: Molecular Biology and Clinical Applications*, pp. 219–231, Plenum Press, New York
16. Lokeshwar, V. B., Iida, N., and Bourguignon, L. Y. W. (1996) *J. Biol. Chem.* **271**, 23853–23864
17. Roden, L., Campbell, P., Fraser, J. R. E., Laurent, T. C., Pertoff, H., and Thompson, J. N. (1989) in *The Biology of Hyaluronan* (Evered, D., and Whelan, J., eds) pp. 60–86, Wiley and Sons, Chichester, UK
18. Knudson, W., Biswas, C., and Toole, B. P. (1984) *Proc. Natl. Acad. Sci. U. S. A.* **81**, 6767–6771
19. Pauli, B. U., and Knudson, W. (1988) *Hum. Pathol.* **19**, 628–639
20. Delpech, B., Chevallier, B., Reinhardt, N., Julien, J. P., Dival, C., Maingonnat, C., Bastit, P., and Asselain, B. (1990) *Int. J. Cancer.* **46**, 388–390
21. Liu, D., Pearlman, E., Guo, E. D. K., Mori, H., Haqqi, S., Markowitz, S., Willson, J., and Sy, M. S. (1996) *Proc. Natl. Acad. Sci. U. S. A.* **93**, 7832–7837
22. Lokeshwar, V. B., Lokeshwar, B. L., Pham, H. T., and Block, N. L. (1996) *Cancer Res.* **56**, 651–657
23. Pham, H. T., Block, N. L., and Lokeshwar, V. B. (1997) *Cancer Res.* **57**, 778–783
24. Lokeshwar, V. B., Young, M. J., Goudarzi, G., Iida, N., Yudin, A. I., Cherr, G. N., and Selzer, M. G. (1999) *Cancer Res.* **59**, 4464–4470
25. Ponting, J., Rooney, P., and Kumar, S. (2002) *Current Perspectives in Molecular and Cellular Oncology*, Jai Press, New York, in press
26. Hall, C. L., Lange, L. A., Prober, D. A., Zhang, S., and Turley, E. A. (1996) *Oncogene* **13**, 2213–2224
27. Rao, C. M., Deb, T. B., and Datta, K. (1996) *Biochem. Mol. Biol. Int.* **40**, 327–337
28. Fieber, C., Plug, R., Sleeman, J., Dall, P., Ponta, H., and Hoffmann, M. (1999) *Gene (Amst.)* **226**, 41–50
29. Serbulea, M., Kakumu, S., Thany, A. A., Miyazaki, K., Machida, K., Senga, T., Ohta, S., Yoshioka, K., Hotta, N., and Hamaguchi, M. (1999) *Int. J. Oncol.* **14**, 733–738
30. Fitzgerald, K. A., Bowie, A. G., Skeffington, B. S., and O'Neill, L. A. J. (2000) *J. Immunol.* **164**, 2053–2063
31. Slevin, M., Krupinski, J., Kumar, S., and Gaffney, J. (1998) *Lab. Invest.* **78**, 987–1003
32. Nandi, A., Estess, P., and Siegelman, M. H. (2000) *J. Biol. Chem.* **275**, 14939–14948
33. Lokeshwar, V. B., and Selzer, M. G. (2000) *J. Biol. Chem.* **275**, 27641–27649
34. Trochon, V., Malibat, C., Bertrand, P., Legrand, Y., SmadjaJoffe, F., Soria, C., Delpech, B., and Lu, H. (1996) *Int. J. Cancer.* **66**, 664–668
35. Rooney, P., Kumar, S., Ponting, J., and Wang, M. (1995) *Int. J. Cancer.* **60**, 632–636
36. Rooney, P., and Kumar, S. (1993) *Differentiation* **54**, 1–9
37. Lauder, H., Sellers, L. A., Fan, T. P. D., Feniuk, W., and Humphrey, P. P. A. (1997) *Br. J. Pharmacol.* **122**, 663–670
38. Shea, T. B., Perrone-Bizzozero, N. I., Beermann, M. L., and Benowitz, L. I. (1991) *J. Neurosci.* **11**, 1685–1690
39. Yassin, R. R., and Abrams, J. T. (1998) *Peptides* **19**, 47–55
40. Vainikka, S., Joukou, V., Wennistrom, S., Bergman, M., Pelicci, P., and Alitalo, K. (1994) *J. Biol. Chem.* **269**, 18320–18326
41. Coussens, L., Parker, P. J., Rhee, L., Yang-Feng, T. L., Chen, E., Waterfield, M. D., Francke, U., and Ullrich, A. (1986) *Science* **233**, 859–866
42. McCaffery, R. E., Coggins, L. W., Doherty, I., Kennedy, I., O'Prey, M., McColl, L., and Campo, M. S. (1989) *Oncogene* **4**, 1441–1448
43. Xia, P., Aiello, L. P., Ishii, H., Jiang, Z. Y., Park, D. J., Robinson, G. S., Takagi, H., Newsome, W. P., Jirousek, M. R., and King, G. L. (1996) *J. Clin. Invest.* **98**, 2018–2026
44. Farese, R. V., and Cooper, D. R. (1991) in *Lipid-related Second Messengers* (Siddle, K., and Hutton, J. C., eds) pp. 205–206, IRL Press Ltd., Oxford, UK
45. Szekeres, C. K., Tang, K., Trikha, M., and Honn, K. V. (2000) *J. Biol. Chem.* **275**, 38831–38841
46. Kim, C. G., Park, D., and Rhee, S. G. (1996) *J. Biol. Chem.* **271**, 21187–21192
47. Allen, V., Swigart, P., Cheung, R., Cockcroft, S., and Katan, M. (1997) *Biochem. J.* **327**, 545–552
48. Gschwendt, M., Dieterich, S., Rennecke, J., Kittstein, W., Mueller, H. J., and Johannes, F. J. (1996) *FEBS Lett.* **392**, 77–80
49. Yedovitzky, M., MochlyRosen, D., Johnson, J. A., Gray, M. O., Ron, D., Abramovitch, E., Cerasi, E., and Neshher, G. (1997) *J. Biol. Chem.* **272**, 1417–1420
50. Lerner, E. C., Qian, Y., Blaskovich, M. A., Fossum, R. D., Vogt, A., Sun, J., Cox, A. D., Der, C. J., Hamilton, A. D., and Sebt, S. M. (1995) *J. Biol. Chem.* **270**, 26802–26806
51. AbdAlla, S., Lother, H., and Quitterer, U. (2000) *Nature.* **407**, 94–98
52. Van Biesen, T., Hawes, B. E., Raymond, J. R., Luttrell, L. M., Koch, W. J., and Lefkowitz, R. J. (1996) *J. Biol. Chem.* **271**, 1266–1269
53. Mukai, H., Muneakata, E., and Higashijima, T. (1992) *J. Biol. Chem.* **267**, 16237–16243
54. Bourguignon, L. Y. W., Zhu, H. B., Shao, L. J., and Chen, Y. W. (2001) *J. Biol. Chem.* **276**, 7327–7336
55. Vanderkuur, J. A., Butch, E. R., Waters, S. B., Pessin, J. E., Guan, K., and Carter-Su, C. (1997) *Endocrinology* **138**, 4301–4307
56. Noh, D.-Y., Shin, S. H., and Rhee, S. G. (1995) *Biochim. Biophys. Acta* **1242**, 99–114
57. Luttrell, L. M., van Biesen, T., Hawes, B. E., Koch, W. J., Kreuger, K. M., Touhara, K., and Lefkowitz, R. J. (1997) *Adv. Second Messenger Phosphoprotein Res.* **31**, 263–277
58. Schwindinger, W. F., and Robishaw, J. D. (2001) *Oncogene* **20**, 1653–1660
59. Jeay, S., Sonenshein, G. E., Kelly, P. A., Postel-Vinay, M. C., and Baixeras, E. (2001) *Endocrinology* **142**, 147–156
60. Kim, I., Moon, S. O., Kim, S. H., Koh, Y. S., and Koh, G. Y. (2001) *J. Biol. Chem.* **276**, 7614–7620
61. Hodson, E. A. M., Ashley, C. C., and Lynn, J. S. (1999) *Biochem. Biophys. Res. Commun.* **258**, 425–430
62. Thodeti, C. K., Adolfsson, J., Juhas, M., and Sjolander, A. (2000) *J. Biol. Chem.* **275**, 9849–9853
63. Satoh, T., Nakafuku, M., and Kaziro, Y. (1992) *J. Biol. Chem.* **267**, 24149–24152
64. Takai, Y., Sasaki, T., and Matozaki, T. (2001) *Physiol. Rev.* **81**, 153–208
65. Garbay, C., Liu, W. Q., Vidal, M., and Rogues, B. P. (2000) *Biochem. Pharmacol.* **60**, 1165–1169
66. Bourguignon, L. Y. W., Zhu, H. B., Zhu, H., Diedrich, F., Singleton, P. A., and Hung, M. C. (2001) *J. Biol. Chem.* **276**, 48679–48692
67. Harrington, E. O., Doyle, K. E., Brunelle, J. L., and Ware, J. A. (2000) *Biochem. Biophys. Res. Commun.* **271**, 499–508
68. Wellner, M., Maasch, C., Kupprion, C., Lindschau, C., Luft, F. C., and Haller, D. (1999) *Arterioscler. Thromb. Vasc. Biol.* **19**, 178–185
69. Yasunari, K., Kohno, M., Kano, H., Minami, M., and Yoshikawa, J. (2000) *Hypertension* **35**, 1092–1098
70. Yano, K. J., Bauchat, J. R., Liimatta, M. B., Clemmons, D. R., and Duan, C. M. (1999) *Endocrinology* **140**, 4622–4632
71. Volkov, Y., Long, A., and Kelleher, D. (1998) *J. Immunol.* **161**, 6487–6495
72. Hall, C. L., Collis, L. A., Bo, J., Lange, L., McNicol, A., Gerrard, J. M., and Turley, E. A. (2001) *Matrix Biol.* **20**, 183–192
73. Ohta, S., Yoshida, J., Iwata, H., and Hamaguchi, M. (1997) *Int. J. Oncol.* **10**, 561–564
74. Skubitz, K. M., Campbell, K. D., and Skubitz, A. P. N. (1998) *FEBS Lett.* **439**, 97–100
75. Zhang, S., Chang, M. C. Y., Zylka, D., Turley, S., Harrison, R., and Turley, E. A. (1998) *J. Biol. Chem.* **273**, 11342–11348
76. Tsifrina, E., Ananyeva, N. M., Hastings, G., and Liau, G. (1999) *Am. J. Pathol.* **155**, 1625–1633
77. Camenisch, T. D., and McDonald J. A. (2000) *Am. J. Respir. Cell Mol. Biol.* **23**, 431–433
78. Savani, R. C., Caos, G., Pooler, P. M., Zaman, A., Zhou, Z., and DeLisser, H. M. (2001) *J. Biol. Chem.* **276**, 36770–36778